University of Szeged
Albert Szent-Györgyi Center for Medical and Pharmaceutical Sciences
Department of Neurology

PARP ACTIVATION AND INFLAMMATORY REACTION IN SELECTIVE NEURODEGENERATION

Ph.D. Thesis
by

Judit Soós, M.D.

2007

Supervisor:
József I. Engelhardt, M.D., D.Sc.
Professor of Neurology

PUBLICATIONS RELATED TO THE THESIS

I. Soós J, Engelhardt JI, Siklós L, Havas L, Majtényi K.
The expression of PARP, NF-κB and parvalbumin is increased in Parkinson disease. NeuroReport 6; 15: 1715-8 (2004). IF: 2.591

II. Kim SH, Engelhardt JI, Henkel JS, Siklós L, Soós J, Goodman C, Appel SH. Widespread increased expression of the DNA repair enzyme PARP in brain in amyotrophic lateral sclerosis. Neurology 62: 319-322 (2004). IF: 5.340

III. Engelhardt JI, Soós J, Obál I, Vígh L, Siklós L. Subcellular localization of IgG from the sera of ALS patients in the nervous system. Acta Neurol Scand 112: 126-133 (2005). IF: 1.712

Abbreviations

6-OHDA	6-hydroxydopamine
AD	Alzheimer's disease
ALS	amyotrophic lateral sclerosis
AMPA	alpha-amino-3-hydroxy-5-methyl-4-isoxazolepropionic
acid	
AP-1	activator protein-1
AR-JP	autosomal recessive juvenile parkinsonism
AT	axon terminal
ATP	adenosine triphosphate
C1,-3,-5	complement-1, -3, -5
Ca^{2+}	calcium
CNS	central nervous system
COX-2	cyclooxygenase-2
CSF	cerebrospinal fluid
Cu/Zn SOD	Cu/Zn superoxide dismutase
DA	dopamine
DAB-3,3'	diaminobenzidine tetrahydrochloride-3,3'
DLBD	diffuse Lewy body disease
EAAs	excitatory amino acids
EAAT2	excytarory amino acid transporter
EC	endothelial cell
FALS	familial ALS
FPD	familial Parkinson disease
GFAP	glial fibrillary acidic protein
ICAM-1	intercellular adhesion molecule-1
IFN-γ	interferon-gamma
IgG	immunoglobulin G
IL	interleukin
iNOS	inducible nitric oxide synthase
ip	intraperitoneal
KA	kainate

LMN	lower motor neuron
Mit	mitochondrion
MN	motor neuron
MPTP	1-methyl-4-phenyl-1,2,3,6-tetrahydropyridine
My	myelin
NAD^+	nicotinamide adenine dinucleotide
NF	neurofilament
NF-κB	nuclear transcriptional factor kappa B
NMDA	N-methyl-D-aspartate
nNOS	neuronal nitric oxide synthase
N	nucleus
NO	nitric oxide
$ONOO^-$	peroxynitrite
PARP	poly-ADP-(ribose)-polymerase
PARP-IR	PARP immunoreactivity
PBS	phosphate-buffered saline
PD	Parkinson disease
RER	rough endoplasmic reticulum
ROS	reactive oxygen species
SALS	sporadic ALS
SN	substantia nigra
SV	synaptic vesicles
TGF	transforming growth factor
TNF-R1	TNF-α receptor
TNF-α	tumor necrosis factor alpha
UCH-L1	ubiquitin carboxy terminal hydrolase-L1
UMN	upper motor neuron

Contentents

1. Introduction

Parkinson disease (PD) and amyotrophic lateral sclerosis (ALS) are devastating neurodegenerative diseases which ultimately lead to death. While the clinical course and the signs of the diseases are totally different, they have a common feature; the selective neuronal death. In ALS, there is a loss of upper motor neurons (UMNs - cortical) and lower motor neurons (LMNs - spinal, bulbar, and pontine), whereas in PD the selective death of DA-ergic neurons in the substantia nigra (SN) is the main feature. Several lines of experimental evidence have proved the combined role of genetic defects, environmental factors, oxidative stress, immune/inflammatory reactions, excitatory mechanisms, and overactivation of the DNA repair enzyme the poly-ADP-(ribose)-polymerase (PARP) in selective neuron degeneration. It is still unknown which one of the proposed mechanisms is the initiator of the selective neuronal death.

1.1. Parkinson disease

PD is a neurodegenerative movement disorder characterized by hypokinesia, rigidity, resting tremor and postural instability. The pathological hallmarks of the disease are Lewy body inclusions in the DA-ergic cells and a selective and progressive loss of the DA-ergic cells in the SN. The forms of PD include the relatively rare, early-onset familial PD (FPD) and a late-onset, sporadic PD form. Specific mutations have been identified in at least five separate genes and linked to different forms of FPD. The discovery of alpha-synuclein, ubiquitin C-terminal hydrolase, parkin, tau and DJ1 (PARK7) mutations and analysis of the biochemical and molecular properties of these gene products point to the critical role of protein aggregation in the degeneration of the DA-ergic neurons of the SN. Even in sporadic PD the Lewy bodies contain some of these gene products, and particularly abundant fibrillar alpha-synuclein. However, in sporadic PD, the causes of the cell demise remain unknown. The neurodegeneration may result from a decreased activity of the proteasome. A defect in the detoxification of reactive oxygen species (ROS), or an energy failure caused by inhibition of the mitochondrial respiratory chain at the level of complex I, or caused by overactivation of the DNA repair enzyme, PARP, are other hypotheses that are described in the literature. Finally, activated microglial cells around the degenerating DA-ergic neurons and complex immune-inflammatory processes might also intervene in the mechanism of

degeneration by perpetuating or amplifying, and (according to some authors) even initiating the primary neuronal insult.

It is still unclear which of the presumed factors and what extent are responsible for the degeneration of the DA-ergic neurons. There are several possibilities: genetic factors, environmental, endogenous risk factors, a mitochondrial dysfunction, or oxidative damage summarized bellow.

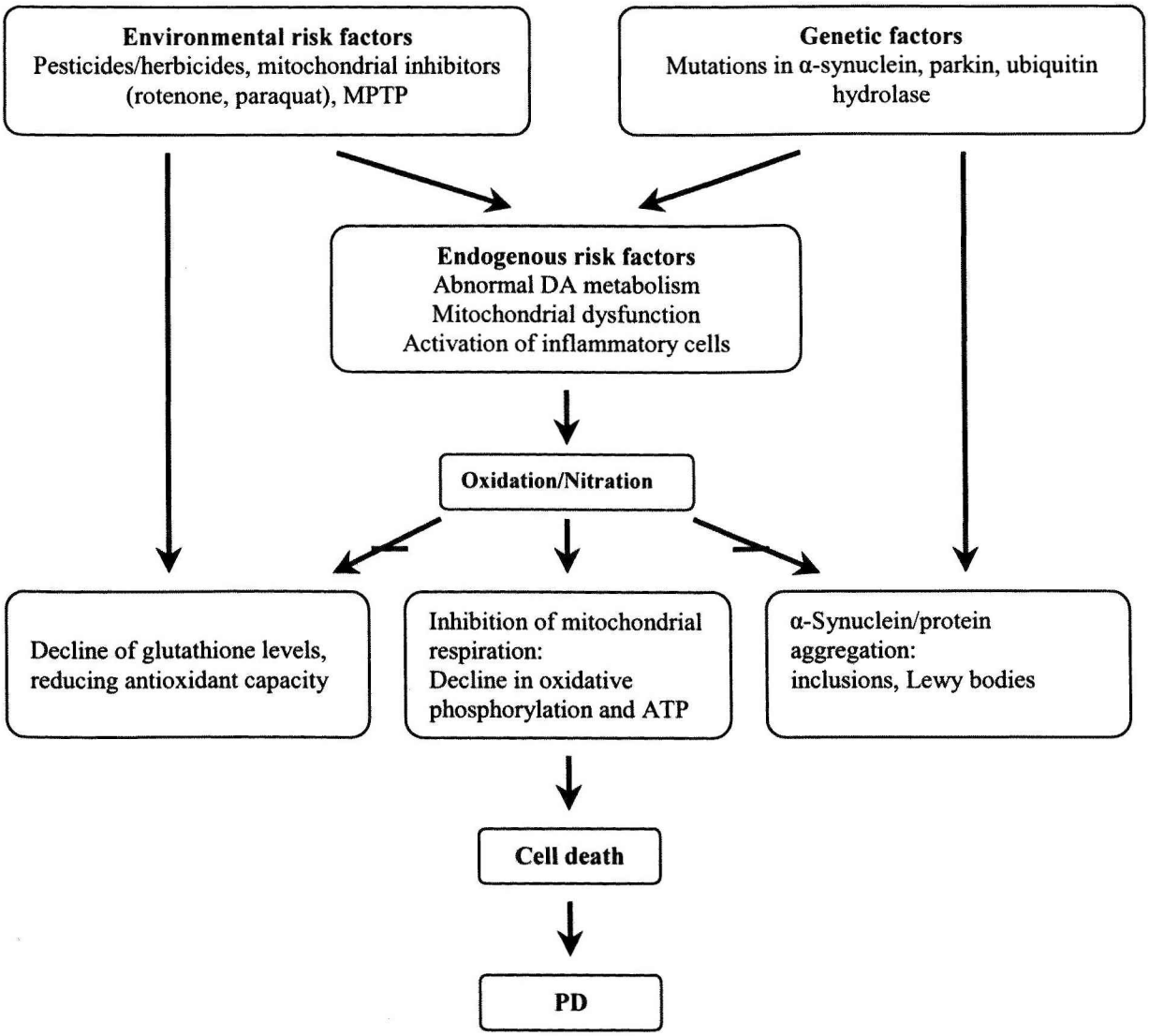

1.1.1. The genetic factors

Genetic analyses have identified three causative genes: PARK1 (*alpha-synuclein*), PARK2 (*parkin*), and PARK7 (*DJ-1*). Additionally, mutations in several other genes have been implicated in familial PD. Deletions or point mutations in the gene for parkin cause autosomal recessive juvenile parkinsonism (AR-JP). Moreover, it is known that the role of parkin protein in the brain is to break down misfolded proteins via the proteosomal pathway as an ubiquitin-protein ligase. It is hypothesized that loss of this function results in the toxic accumulation of its target proteins. Disturbance of protein degradation by the ubiquitin-proteasome system may have a critical role in neurodegeneration. Although alpha-synuclein mutations are infrequent, alpha-synuclein accumulates in Lewy bodies, and alpha-synuclein fibrils impair the 26S proteasome function. Ubiquitin carboxy-terminal hydrolase-L1 (UCH-L1) is also an abundant deubiquitinylating enzyme, and its mutation is linked to PARK5. Another PD causative gene, DJ-1 functions as a sensor for oxidative stress (1). Most of the genes found to be mutated in PD have played a role in the ubiquitin–proteasome system.

There is much evidence of decreased enzymatic activity in the affected parts of the brains of patients with AR-JP. Mutations in parkin lead to an accumulation of nonubiquitinated proteins in DA neurons. The impairment of the ubiquitin-proteasome system and the resulting toxicity of poorly degraded proteins could be the cause of PD in these individuals. DJ-1 is similarly involved in the ubiquitin-proteasome pathway for two reasons. First, mutations leading to misfolded DJ-1 might overload the ubiquitin-proteasome system and decrease its effectiveness. Second, DJ-1 is thought to be involved in oxidative damage, which is known to increase the rate of aggregation of alpha-synuclein. Alpha-synuclein, however, is not limited strictly to DA-ergic neurons, and therefore its accumulation can not fully explain the specificity seen in the disease.

In the non-genetic forms of PD, there is also well-known DNA damage caused in the DA-ergic neurons by toxins, oxidative stress. The DNA breaks activate its repair enzyme PARP. The latter also has an important role in the pathomechanism of sporadic PD.

1.1.2. Environmental risk factors

The theory that exposure to some toxins may contribute to nigrostriatal neuronal death was a result of the accidental intoxication of drug users by 1-methyl-4-phenyl-1,2,3,6-tetrahydropyridine (MPTP), which was a contaminant of street drugs. People intoxicated with MPTP presented with a sudden onset of all the symtoms of PD, although with less tremor and more cognitive impairment, drooling and balance difficulty. The pathologic hallmarks characteristic of PD, namely the Lewy bodies, were not seen in experimental PD induced in primates by MPTP. Several chemical products used in herbicides and pesticides are similar structurally to MPTP, including paraquat, diquat and rotenone. In view of this fact, some animal models were developed for the selective nigrostriatal damage, such as neurotoxicity induced by rotenone, paraquat or MPTP, which emphasised that environmental agents may conduce to the neurodegenerative process in PD. There is a link between MPTP toxicity and PARP activation because MPTP potently activates PARP exclusively in vulnerable DA-containing neurons of the SN. MPTP elicits a novel pattern of poly-(ADP-ribosyl)-ation of nuclear proteins that completely depends on neuronally derived nitric oxide (NO). NO, DNA damage and PARP activation play critical roles in MPTP-induced parkinsonism and suggest that inhibitors of PARP may be of protective benefit in the treatment of PD (2).

1.1.3. Oxidative stress

Oxidative stress has been proposed as one of several pathogenic hypotheses in PD. Oxidative stress is a unifying factor in the current theories of PD pathogenesis, because it links genetic and potential environmental factors (mitochondrial inhibitors such as rotenone, paraquat and MPTP) to the initiation of the disease process.

Oxidative stress is intimately linked to other components of the degenerative process, such as a mitochondrial dysfunction, excitotoxicity, toxicity by NO and inflammation.

MPTP administration has been shown to increase levels of superoxide both intracellularly, via the inhibition of mitochondrial respiration, and extracellularly, via the activation of microglia. Microglial activation is regulated in part by nuclear transcription factor (NF-κB). The nuclear enzyme PARP-1 enhances NF-κB binding to DNA. PARP-1 activity is necessary for its function as a coactivator of NF-κB.

Pharmacological PARP inhibitors have been shown to block the effect of PARP-1 on NF-κB binding to DNA. Superoxide and NO production by neuronal NO synthase (nNOS) or by microglial inducible NO synthase (iNOS) also contributes to MPTP neurotoxocity.

There is increasing evidence that mitochondrial function impairment, oxidative damage and inflammation are factors contributing to neurodegeneration. A defect in the detoxification of ROS or an energy failure caused by inhibition of the mitochondrial respiratory chain, at the complex I level, are other hypotheses that are frequently mentioned. Finally, activated microglial cells around the degenerating DA-ergic neurons may also intervene in the mechanism of degeneration by perpetuating or even amplifying the primary neuronal insult. A mitochondrial dysfunction can result in the excessive production of ROS, triggering the apoptotic death of DA-ergic cells in PD.

1.1.4. Excitotoxicity

The main excitatory amino acids (EAAs) are L-glutamate and L-aspartate. The excitatory responses in the central nervous system (CNS) are mediated by four different receptor subtypes. Three of these receptors are coupled to ion channels: the N-methyl-D-aspartate (NMDA), α-amino-3-hydroxy-5-methyl-4-isoxazole-propionate (AMPA), and kainate (KA) receptors. The fourth receptor subtype is linked to the phosphoinositol cascade and is known as the metabotrophic receptor. Studies on the molecular mechanism of neuronal injury caused by excessive stimulation of glutamate receptors showed that glutamate may be toxic to neurons in several ways. The NMDA receptor is coupled with a voltage-gated calcium (Ca^{2+}) channel and its stimulation causes elevated intracellular calcium Ca^{2+} levels. The activation of non-NMDA receptors (AMPA and KA) results in an influx of Na^{+}, followed by an influx of Ca^{2+}. Destabilization of the intracellular Ca^{2+} level activates protein kinases, phospholipases, proteases and NOS, impairs the mitochondrial function, generates free radicals and initiates apoptosis.

In the normal brain, the concentrations of EAAs within the synaptic cleft are maintained at subtoxic levels, with rapid uptake and inactivation by both neurons and glia. Nigral DA-ergic neurons possess glutamate receptors (3, 4) and they degenerate if exposed to an excitotoxic impact of glutamate (6, 7). The antagonism of excitotoxicity has been regarded as potential therapy in PD. Antagonists of ionotropic glutamate receptors, and

especially antagonists of the NMDA receptor and its modulatory glycine site, improve PD symptoms, but severe side-effects associated with their use during chronic therapy limit their efficacy as potential drugs.

High levels of glutamate can be lethal for neurons via secondary excitotoxicity. Mitochondrial impairment also disrupts cellular Ca^{2+} homoeostasis. Facilitation of the NMDA-receptor function leads to a further mitochondrial dysfunction. This largely occurs due to Ca^{2+} entering the neurons through NMDA receptors with 'privileged' access to mitochondria. An elevated intracellular Ca^{2+} level causes free-radical production and mitochondrial depolarization. Glutamate in the presence of an impaired cellular energy metabolism acts as a neurotoxin. In this way, glutamate may participate in the pathogenesis of PD (8, 9).

1.1.5. The role of iron in neurodegeneration

Iron is believed to be a key contributor to PD pathology by inducing the aggregation of alpha-synuclein and by generating oxidative stress. Histopathological, biochemical and brain imaging techniques, such as magnetic resonance imaging and transcranial sonography, have revealed a consistent increase of the brain iron level in the SN in PD. A series of recent studies suggest that iron regulatory proteins coordinate both cellular iron levels and energy metabolism, which are both disrupted in PD. Iron has also recently been implicated in the promotion of alpha-synuclein aggregation, either directly or by increasing levels of oxidative stress, suggesting an important role for it in Lewy body formation, another important hallmark of the disease (10).

1.1.6. Immune/inflammatory theories

The presence of activated microglia in the SN pars compacta in patients with PD has prompted investigations of the role of immune/inflammatory processes in neurodegenerative disorders, including PD. The SN pars compacta contains icreased levels of cytokines, such as tumor necrosis factor alpha (TNF-α), interleukin (IL)-1beta, IL-2, IL-4, IL-6 and transforming growth factor (TGF)-alpha, TGF-beta1 and TGF-beta2. In turn, the levels of neurotrophins, such as brain-derived neurotrophic factor and nerve growth factor, are decreased in the nigrostriatal DA regions and in the ventricular and lumbar cerebrospinal fluid (CSF) of PD patients. Furthermore, the levels of the

TNF-α receptor R1 (TNF-R1), bcl-2, soluble Fas (sFas), and the activities of caspase-1 and caspase-3 are also elevated in the nigrostriatal DA regions in PD (11). Increased levels of proinflammatory cytokines, cytokine receptors, caspase activities, and reduced levels of neurotrophins in the nigrostriatal region in PD patients, and in its animal models (MPTP- and 6-hydroxy-DA-produced PD animals) suggest the increased immune reactivity and programmed cell death (apoptosis) of neuronal cells, alterations in the function of the astrocytes and activation of the microglia. These data indicate a proapoptotic environment in the SN in PD which may induce the increased vulnerability of neuronal cells. The DA-ergic neurons may lack the protection given by the astrocytes. Another possibility is that the microglia cells themselves could contribute to neurodegeneration through an inflammatory process. It is believed that activated microglia exerts cytotoxic effects in the brain through two very different and yet complementary processes (12). First, they can act as phagocytes, which involve direct cell-to-cell contact. Second, they are capable of releasing a large variety of potentially noxious substances, such as iNOS, IL-1β, IL-2, IL-6, IL-10, cyclooxygenase-2 (COX-2), TNF-α, interferon (IFN-γ). (13-15) and glutamate (16). Alternatively, superoxide released by activated microglia can react with NO in the extracellular space to form the highly reactive tissue-damaging species peroxynitrite ($ONOO^-$), which can cross the cell membrane and injure neurons. Therefore, by contributing to peroxynitrite formation, microglia-derived superoxide may participate in the death of DA-ergic neurons. Proinflammatory cytokine TNF-α synthesized predominantly by microglia and astrocytes is an obligatory component of DA-ergic neurodegeneration. TNF-α may link inflammation to apoptosis in PD.

These changes in cytokine and neurotrophin levels may be initiated by activated microglia, which may then promote apoptotic cell death and subsequent phagocytosis of DA neurons (17).

1.1.7. The role of PARP overactivation

PARP-1 is an abundant nuclear protein functioning as a DNA nick-sensor enzyme. Upon binding to DNA breaks, activated PARP cleaves nicotinamide adenine dinucleotide (NAD^+) into nicotinamide and ADP-ribose and polymerizes the latter into nuclear acceptor proteins, including histones, transcription factors and PARP itself.

Poly-(ADP-ribosylation) contributes to DNA repair and to the maintenance of genomic stability. Overactivation of PARP consumes NAD^+ and consequently adenosine triphosphate (ATP), culminating in a cell dysfunction, apoptosis and necrosis. Mild genotoxic noxae cause PARP activation, which facilitates DNA repair and cell survival. Severe DNA damage, however, causes the overactivation of PARP, resulting in the depletion of NAD^+ and ATP and consequently neuronal cell death.

Pharmacological PARP inhibition or the absence of PARP in PARP-deficient mice preserves cellular ATP and NAD^+ pools in oxidatively stressed cells and thereby allows them to function normally (18).

Another role of PARP-1 is noted in the production of inflammatory mediators such as the iNOS (19-21), intercellular adhesion molecule-1 (ICAM-1) (22). NF-κB is a key transcription factor in the regulation of this set of proteins, and PARP has been shown to act as a coactivator in the NF-κB-mediated transcription (23). Oxidative stress generates DNA single-strand breaks. DNA strand breaks then activate PARP, which in turn potentiates NF-κB activation and activator protein-1 (AP-1) expression, resulting in greater expression of the AP-1- and NF-κB-dependent genes, such as iNOS, ICAM-1, macrophage inflammatory protein-1α (MIP-1α), TNF-α and complement 3 (C3). The generation of complement 5a (C5a) in combination with an increased endothelial expression of ICAM-1, recruits a larger number of activated leukocytes to inflammatory foci, producing a higher level of oxidative stress. Overactivation of PARP depletes the energy of the cells, which leads to the reduction of other energy- dependent molecules such as oxidized glutathione, the main intracellular antioxidant. As a consequence of the intracellular energetic failure or devastating oxidant exposure, the depletion of reduced glutathione induces an increased free radical level, resulting in greater DNA strand breakage.

The wide variety of animal models in which PARP inhibition has proved beneficial indicates that PARP inhibitors block a common pathway of tissue injury, such as NF-κB activation or oxidative stress-induced cytotoxicity (24, 25).

1.2. Amyotrophic lateral sclerosis

ALS is the most common form of degenerative MN disease in adulthood. The clinical picture, first described by Charcot 130 years ago, consists of generalized fasciculations,

progressive atrophy and weakness of the skeletal muscles, spasticity and other pyramidal tract signs, dysarthria, dysphagia, dyspnea and speech deficits, which are signs of the degeneration of the upper and lower MNs. The criteria for the diagnosis of ALS, defined in Airlie House, Virginia, USA, in 1998, include clinical, electrophysiological, neuroradiological and pathological signs.

The disorder is often asymmetrical at its onset and the weakness typically begins focally. The onset of symptoms seen in ALS patients is assumed to occur when approximately 60-80% of MNs have been lost. It is a rapidly progressive disease, mostly resulting in death within 1-5 years from onset. The prevalence of the disease increases with age and the male and female ratio is 1.57: 1.

There are two forms of ALS. The sporadic form (SALS) accounts for approximately 90% of the reported cases, while 5-10% are familial (FALS). The cause of SALS is unknown. Twenty per cent of the FALS cases are linked to chromosome 21 and are associated with mutation of the Cu/Zn (superoxide dismutase) SOD gene. At present, more than 130 different mutations in the SOD 1 gene have been reported in FALS patients. These mutations result in reduced Cu/Zn SOD activity *in vitro*, though much evidence suggests a novel gain of function of the enzyme rather than a loss of function. The degree of reduction in its actvity does not correlate with either the age of onset, or the duration or severity of the disease.

Microglia and astrocytes are also involved in the pathological processes (26). Changes in the white matter (loss of axon myelin and fibrillary astrocytosis) are also seen. The function of the MNs innervating the external ocular muscles, the striated urinary and anal sphincter, the abductor muscle of the larynx and the cricopharyngeal sphincter muscles are intact during the course of the disease.

The pathomechanisms of ALS

There are several hypotheses which account for the degeneration of the MNs.

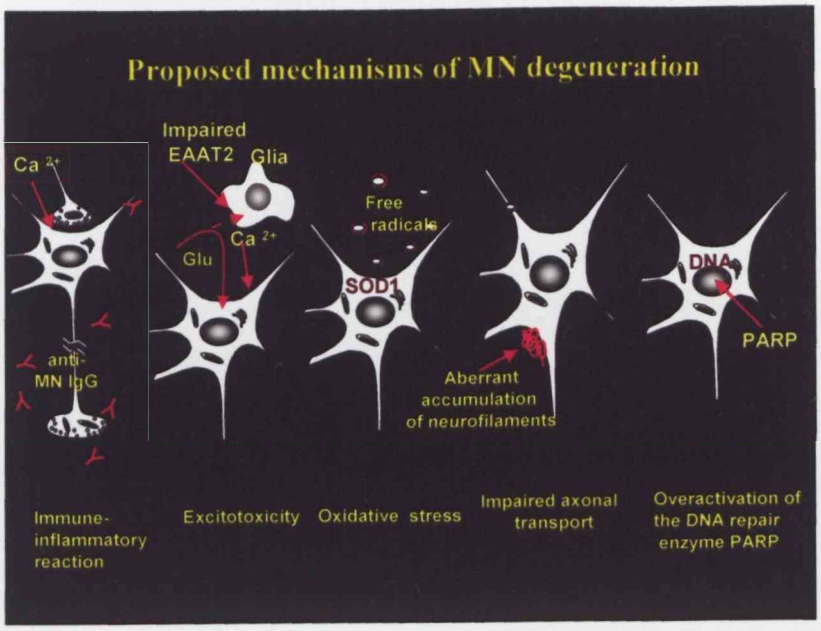

1.2.1. The immune/inflammatory mechanism

The immune/inflammatory reaction in the CNS is characterized by activation and proliferation of microglia and infiltration by T cells and the presence of immunoglobulinG (IgG) in the MNs.

IgG antibodies directed to L-type voltage-gated Ca^{2+} channels were detected in the sera of 75% of SALS patients. ALS IgG binding to the Ca^{2+} channels can alter the function of these channels (L-type and N/P/Q channels) (27). ALS IgG was found to enhance Ca^{2+} currents in the voltage-gated Ca^{2+} channels in motor nerve terminals and to increase acetylcholine release. Accordingly, motor nerve terminals can be the site of immune attack and the increase in intracellular Ca^{2+} may be an early event leading to neuronal injury.

ALS IgG passively transferred to mice induces similar ultrastructural changes in the MNs as observed in patients with SALS (an increased number of synaptic vesicles (SVs), an increased synaptic mitochondrial volume, swelling and fragmentation of the Golgi apparatus outer leaflet, and an increased Ca^{2+} concentration in the mitochondria, the Golgi apparatus and the endoplasmic reticulum. Furthermore, an increased Ca^{2+} concentration and vesicle density in terminals contacting LMNs, and increased glutamate release from them, have also been observed (28). In the motor cortices of ALS patients, IgG was found in the pyramidal MNs. The intraperitoneal (ip) injection of ALS IgG results in a much greater uptake of IgG in MNs than does the injection of

disease control IgG. Other experiments have demonstrated that the cell death mediated by ALS IgG is triggered by a transitory increase in intracellular Ca^{2+}.

Besides the presence of IgG, microglia activation has been demonstrated in the area of the neuronal damage. The microglia may play three possible roles: 1. phagocytosis of injured MNs, 2. participation in the injury, and 3. an attempt to repair the damage (29, 30). The first and second roles have been proved; the third is only assumed in ALS.

The microglia is prominent around the UMNs and LMNs and in the degenerating corticospinal tracts. They play important roles as mediators of immune/inflammatory reactions. Around the MNs, they can proliferate and become activated. Activated microglia cells are competent antigen-presenting cells (31) and may play a role in the recognition, uptake, processing, and presentation of antigens in the CNS. They are able to produce neurotoxic cytokines and free radicals (32-35), TNF-α, glutamate and iNOS.

1.2.2. Excitotoxicity

There are several lines of evidence that support the involvement of excitotoxic mechanisms in the pathogenesis of ALS. Glutamate is the major excitatory neurotransmitter in the CNS. UMNs projecting to LMNs are assumed to be glutamatergic, and consequently postsynaptic MNs possess a high density of glutamate receptors. An increased glutamate level in the synaptic cleft could induce the overexcitation of LMNs, leading to an excessive influx of Ca^{2+}.

The AMPA and KA receptors are thought to be the mediators of fast excitatory neurotransmission. The majority of these receptors are permeable only to Na^{+} and K^{+}. The AMPA receptors are formed from four different subunits (GluR1- GluR4). However, if the GluR2 is lacking, the receptors become permeable to Ca^{2+}. A low expression of the GluR2 protein subunit (36) and decreased levels of the mRNA for GluR2 (37) are detected in the MNs of ALS patients.

Glutamate is removed from the synaptic cleft by different uptake mechanisms. Within the glial cells, glutamate is either transaminated by glutamine synthetase to form glutamine or metabolized to α-ketoglutarate by glutamate dehydrogenase. The astrocyte then supplies the nerve terminal with glutamine α-ketoglutarate, or both. These are the precursors of the neurotransmitter glutamate. In this way, glutamate is recycled from the nerve terminal to the glial cells and back to the nerve terminal.

Several EAA transporters (EAATs2) participate in the process of glutamate recycling; they are located on both glial and neuronal cells. Reduced levels of astroglia-specific EAAT2 have been reported in the motor cortex and spinal cord in the majority of ALS patients (38). This finding may explain the elevated glutamate level in the CSF of the patients. The elevated glutamate level may reflect the altered function of the astrocytes, which means that the astrocytes may also be involved in the pathomechanisms of neuronal death.

1.2.3. Oxidative stress

ROS generated during oxidative reactions can induce cellular damage through the oxidation of proteins, lipids and nucleic acids. If the generation of ROS exceeds the scavenging capacity of the cell, because of the increased ROS production or the loss of cellular antioxidant defense systems, oxidative stress prevails. Oxidation-induced damage has been demonstrated in human SALS and FALS and in transgenic mice overexpressing a mutant SOD1 gene. The SOD1 enzyme gains a novel cytotoxic function in MN degeneration (39). One possible explanation is that the mutation affects the conformation of the protein and it becomes more accessible to substrates other than superoxide, such as hydrogen peroxide and $ONOO^-$, from which it generates nitronium ions. Nitronium ions cause the nitration of tyrosine residues and oxidatively damage proteins, lipids and DNA (40). Increased markers for oxidative damage to nucleic acid (8-hydroxy-2'-deoxyguanosine), to proteins (carbonyl proteins) and to lipids (4-hydroxynonenal) have been found in FALS and SALS patients and SOD1 G93A transgenic mice. Neurofilaments (NFs) are further targets for nitrosylation (41). The mutated SOD1 is a source of toxic ROS rather than a scavenger. Cell lines overexpressing a mutant SOD1 gene are known to display enhanced sensitivity to oxidative stress (42).

There may be a link between the oxidative stress induced by mutant SOD1 and glutamate-induced cell death. Free radicals can damage the glial glutamate transporter (EAAT2), inducing excessive glutamatergic stimulation in consequence of the insufficient clearance of glutamate from the synaptic cleft. Oxidative stress leads to the formation of toxic intermediates such as 4-hydroxynonenal, which impairs glutamate transport and induces secondary excitotoxic neurodegeneration. Another link may be

that free radicals damage the mitochondria, resulting in a decreased production of ATP. The activation of PARP by DNA damage enhances this energy deficit by consuming its substrate, NAD^+. This energy failure compromises the function of ATP-dependent ion pumps. The insufficient clearance of Ca^{2+} that enters the cell through stimulation of the glutamate receptors induces an increase in Ca^{2+} level intracellularly, which initiates a variety of enzymatic proccesses leading to cell death. Small vacuoles filled with Ca^{2+} have been observed in the spinal MNs of mutant SOD 1 G93A mice (43), and increased intracellular Ca^{2+} has been found in the motor axon terminals of patients with sporadic ALS (44). Finally, the formation of protein aggregates of mutant SOD1 seems to be dependent on Ca^{2+} entry induced by glutamate stimulation, providing another link between these two mechanisms. The presence of very similar oxidative damage in FALS and SALS suggests that the mechanism of MN degeneration may involve oxidative stress, independently of the primary etiology. PARP-dependent microglia activation is known to be the source of a large amount of free radicals, damaging the neighboring neurons. This can be the other main source of a free radical excess in the tissue.

1.2.4. The role of NF accumulation in neurodegeneration

NF proteins form a major component of the neuronal cytoskeleton and have important functions, including the maintenance of cell shape, axonal caliber and axonal transport. In the perikaryon of the cells, they are composed of three subunits with different molecular weights (NF-heavy, NF-medium and NF-light) and are transported down the axon, while being phosphorylated. NF proteins are potential targets for injury in ALS by nitration of their tyrosine residues. Peroxynitrite, formed from NO and superoxide, may affect NF assembly and cause NF accumulation in the MNs. NF aggregates are tightly linked to SOD-1 and NOS activities. Both enzymes may contribute to peroxynitrite formation at light NFs, which are rich in both tyrosine and arginine residues and hence regarded as the vulnerable site for nitrotyrosine formation. Nitrotyrosine is known to inhibit phosphorylation and, if it impairs the phosphorylation of NF subunits, either light or heavy, it may alter the slow axonal transport, culminating in the accumulation of NF and slowly progressive MN death. NF accumulations in mice are accompanied by proximal axon swellings, an MN dysfunction, and atrophy of the skeletal muscle, but

these mice do not exhibit MN death. There is a link between excitotoxicity and aberrant NF accumulation, because excitoxicity can induce NF side-arm hyperphosphorylation and this slows NF transport in cultured neurons (45).

Free radicals also can induce abnormal aggregations (46). These pathomechanisms are strongly correlated.

1.2.5. The importance of PARP

The activation of PARP in MN degeneration may involve similar principles as in the degeneration of DA-ergic cells in the SN in PD: DNA damage and an elevated intra-motoneuronal Ca^{2+} level. The later is the direct effect of autoimmune IgG directing to Ca^{2+} channels of MNs. Ca^{2+} promotes the activation of PARP, and Ca^{2+} is an activating factor in PARP-mediated cell killing (47, 48). Although PARP is also a well-known DNA repair enzyme, it helps cells to recover after injury. Excessive PARP activation can cause the massive consumption of its substrate NAD^{+}, with a resulting energy failure of the cells, which leads to cell death (49-53).

1.3. The aims of the study

This study was designed to answer the following questions:

- Does the upregulation of PARP play a role in the selective damage of MNs in ALS?
- Is the increase of PARP involved in the selective damage of the DA-ergic neurons of the SN in PD?
- What are the possible mechanisms of neuronal damage involving PARP overactivation?
- Is PARP upregulation restricted to the neurons that are damaged selectively or it is also upregulated in other neurons?
- Is it restricted to neurons, or is it upregulated in microglial cells and astrocytes?
- How does the upregulation of PARP influence the immune-inflammatory reaction in neurodegenerative disease?
- What is the localization of autoimmune IgG from ALS patients in the spinal MNs after passive transfer to mice and in the autopsy tissue from ALS patients?
- What is the possible role of autoimmune IgG in MN degeneration and its connection with PARP activation?

2. Materials and methods

2.1. Postmortem tissue from SALS, PD and control patients

The SALS **brain** (motor cortex, parietal cortex and cerebellum) and **spinal cord** specimens were obtained at autopsy from SALS patients followed in the MDA/ALS Clinic at the Baylor College of Medicine (n=4) and from the University of Maryland Brain Bank (n=4). Postmortem samples of brains from age-matched individuals without neurological diseases (n =6) and from a patient with Alzheimer's disease (AD) were used as controls. The clinical diagnoses were confirmed pathologically in all cases. There was no significant difference between the times from death to autopsy in the SALS and control groups (8.0 ± 2.6 h and 10.2 ± 3.5 h, respectively). Additionally, there was no significant difference between the ages at death (SALS 59.5 ± 5.0 years, controls 50.3 ± 8.5 years). In the SALS group, the cause of death was respiratory failure (n =8). In the control group, the cause of death was a traffic accident (3), acute drug poisoning, or sudden death of unknown cause (2 cases). The AD case died of hypostatic pneumonia.

The **SN** pars compacta was examined in 5 patients who had died of PD and 2 patients who had died of diffuse Lewy body disease (DLBD), and the results were compared with those on the same structure in normal (n=1), ALS (n=1), atherosclerotic (n=1) and AD brains (n=4). The age, gender and *post mortem* interval before the autopsies were matched. The diagnoses were established clinically and confirmed by neuropathological examinations.

To visualize human IgG, approximately 6-mm^3 pieces of the **ventral horns of the lumbar spinal cords** of 5 consecutively deceased ALS patients and 5 controls (who had died from AD, PD, an ischemic stroke, a myocardial infarction, or a pulmonary embolism) were also dissected and fixed in the same fixative, with a 3-day immersion.

2.2. The preparation of IgG

For IgG purification, the blood was obtained by phlebotomy after overnight fasting from 5 patients with clinically definite (54) and pathologically proved sporadic ALS and from 5 controls (one each with AD, PD, Guillain-Barré syndrome or ischemic stroke, and one healthy blood donor), with their informed consent. The IgG was purified

from the sera with AvidChrom-Protein A Kit Pure-1 according to the instructions of the manufacturer (Sigma Bio Sciences, Sigma Chemical Company, St Louis, MO, USA).

2.3. Animal experiments

Forty mg of purified IgG from each sample was injected ip into 3 mice on 2 successive days. Forty-eight h after the first injections, the animals were anesthetized with ketamine-xylasine (87 and 13 mg/kg, respectively), and perfused transcardially with phosphate-buffered physiological saline (PBS) and fixative consisting of 4% paraformaldehyde, 0.05% glutaraldehyde and 0.2% picric acid (55). The lumbar enlargements of the spinal cords and interosseous muscles from the hind limbs were removed and kept in the same fixative for 3 days at 4 °C. The spinal cords were then chopped into 3 mm segments and the ventral horns were dissected. The muscle samples from the vicinity of the terminating nerve branches were also dissected under a stereomicroscope.

Tissue samples were processed either for immunocytochemistry, western blotting or electron microscopic investigations. 32 μm sections thick were cut with a vibratome and processed free floating in different incubation solutions at 4 °C on a rocker to visualize human IgG. After washing in PBS, the sections were preincubated with 5% normal goat serum in PBS for 3 h to saturate the nonspecific IgG-binding sites. The sections were then incubated overnight with a 1:200 dilution of a biotinylated affinity-purified IgG fraction of goat antiserum to human IgG (heavy and light chain-specific) (Organon Teknika, Cappel, West Chester, PA), in 3% normal goat serum containing PBS. As a method control for the immunohistochemical labeling of human IgG, the biotinylated goat IgG directing to human IgG was omitted from the process or replaced with unlabeled antibody. After thorough washing in PBS, the sections were divided into two groups containing equal numbers of sections. One group was incubated with a 1:200 dilution of peroxidase-conjugated avidin (Organon Teknika, Cappel, West Chester, PA) while the other group was incubated with a 1:200 dilution of streptavidin-ferritin conjugate (Bethesda Research Laboratories) for 6 h at 4 °C. After washing in PBS, the sections labeled with peroxidase were exposed to 0.025% Sigma Fast™ 3,3'-diaminobenzidine tetrahydrochloride (DAB) (Sigma Chemical Company, St. Louis, MO) and 0.016% hydrogen peroxide (Fisher Scientific, Pittsburgh, PA) in PBS for 10

min. After washing, 10 sections of the spinal cord of each animal were put on glass slides, dehydrated in series of ethanol, cleared in xylene, mounted in Permount, coverslipped and examined in a Nikon Optiphot light microscope.

2.4. Histological processing

2.4.1. Immunohistochemistry for PARP

Representative sections of brains from 2 SALS patients, from 2 normal controls, and from 1 AD patient were immunostained for PARP. Brain specimens were fixed in 10% neutral formaldehyde and routinely embedded in paraffin. From paraffin blocks, sections 5 μm in thickness were cut, deparaffinized in xylene, rehydrated in a descending series of ethanol, rinsed in 10 mM PBS, and then blocked for endogenous peroxidase activity (0.3% H_2O_2 in methanol, 30 min). The sections were rinsed in PBS and placed in Serotec unmasking fluid (Serotec Inc., Raleigh NC) for antigen retrieval in a microwave oven (2 × 5 min at 600 W). The sections were cooled to room temperature, washed in PBS, and blocked for nonspecific IgG binding by incubation with 5% normal horse serum in PBS for 30 min (Vector Laboratories, Burlingame, CA). Mouse monoclonal anti-human PARP antibody (Serotec US, Raleigh, NC), diluted to 1:100 with PBS containing 2% horse serum, was applied at 4 °C, overnight. The sections were rinsed in PBS and incubated with biotin-labeled horse-anti-mouse IgG (diluted 1:200 in PBS containing 2% normal horse serum; Vector Laboratories, Burlingame, CA) for 30 min at room temperature. The sections were rinsed in PBS and incubated with a biotin-avidin complex conjugated to peroxidase for 30 min (Vector Elite kit; Vector Laboratories, Burlingame, CA). The sections were again rinsed in PBS and developed using the ImmunoPure metal-enhanced DAB substrate kit for 15 min (Pierce, Rockford, IL). The peroxidase reaction was terminated by extensive washing in distilled water. Finally, sections were dehydrated in a graded series of ethanol, cleared in xylene and coverslipped with Permount (Fisher Scientific, Fair Lawn, NJ). As a negative control, the primary antibody (mouse monoclonal anti-human PARP) was omitted from the reaction or was replaced with a 1:100 dilution of normal mouse serum. Several sections were chosen for double immunostaining for both PARP and glial fibrillary acidic protein (GFAP) to verify that PARP-positive nuclei also belong to astrocytic cells. For this purpose, some of the sections that had been stained for PARP

were preincubated in 5% normal goat serum for 1 h at room temperature and then incubated overnight with a 1:800 dilution of polyclonal rabbit antibody directed to bovine GFAP (DAKO A/S, Denmark) containing 3% normal goat serum. After washing in PBS, the sections were incubated for 1 h in a 1:200 dilution of biotinylated anti-rabbit IgG at room temperature and subsequently exposed to Vector ABC Elite reagent (Vectors Laboratories, Inc., Burlingame, CA) for 30 min. After washing, the peroxidase reaction was developed with the Vector VIP peroxidase substrate kit for 5 min to visualize GFAP with a purple reaction product. The macrophages were identified by their clear cytoplasm around the nucleus after dissolution of the phagocytized lipids during the process of embedding the material in paraffin. The sections were dehydrated, cleared, and coverslipped as described.

Immunostained sections were examined in a Zeiss Axioskop microscope (Karl Zeiss, Oberkochen, FRG) equipped with a DXC-970-MD CCD camera (Sony Corp., Japan) and a digital image analysis system (Optimas 6.2; Optimas Corp., Bothell, WA).

Normalized PARP protein levels characterizing SALS and control groups were analyzed with a two-tailed Student's t-test (Excel software). Differences were considered statistically significant with p values of less than 0.05.

2.4.2. Immunocytochemistry for PARP, NF-κB and parvalbumin

Deparaffinized and rehydrated sections from the SN from PD patients were subjected to immunohistochemical staining for PARP, NF-κB (56) and parvalbumin. The detecting reagents were a 1:100 dilution of mouse monoclonal anti-human PARP (Serotec, Raleigh, NC), a 1:100 dilution of rabbit polyclonal NF-κB p65 (A) (Santa Cruz Biotechnology Inc., CA) and a 1:1000 dilution of mouse monoclonal anti-parvalbumin (Sigma Chemical Co., St. Louis, MO). For the whole procedure, mouse and rabbit Elite Vectastain ABC kits (Vector Laboratories Inc., Burlingame, CA) were used according to the manufacturer's description. Consecutive sections were immunostained with the three antibodies, and ten sets of three sections were used for evaluation. The sets of sections were cut 150 μm apart from the next set. Several other sections were double-stained to check on the possible co-localization of PARP with NF-κB and with parvalbumin. For this purpose, sections immunostained for PARP and visualized with DAB with a metal enhancer (Sigma Chemical Co, St. Louis, MO) (brown-black color)

were incubated secondarily with the antibody detecting parvalbumin or NF-κB. The second peroxidase reaction product was visualized with VIP substrate kit as a purple color (Vector Laboratories Inc., Burlingame, CA). The immunostained sections were examined in a Zeiss Axioskop microscope equipped with a DXC-970-MD CCD camera (Sony) and a digital image analysis system (Optimas 6.2).

2.3.3. Immunocytochemistry for IgG

32 μm thick sections were cut with a vibratome and processed free floating in different incubation solutions at 4 °C on a rocker to visualize human IgG. After washing in PBS, the sections were preincubated with 5% normal goat serum in PBS for 3 h to saturate the nonspecific IgG-binding sites. The sections were then incubated overnight with a 1:200 dilution of a biotinylated affinity-purified IgG fraction of goat antiserum to human IgG (heavy and light chain-specific) (Organon Teknika, Cappel, West Chester, PA), in 3% normal goat serum containing PBS. As a method control for the immunohistochemical labeling of human IgG, the biotinylated goat IgG directing to human IgG was omitted from the process or replaced with unlabeled antibody. After thorough washing in PBS, the sections were divided into two groups containing equal numbers of sections. One group was incubated with a 1:200 dilution of peroxidase-conjugated avidin (Organon Teknika, Cappel, West Chester, PA), while the other group was incubated with a 1:200 dilution of streptavidin-ferritin conjugate (Bethesda Research Laboratories) for 6 h at 4 °C. After washing in PBS, the sections labeled with peroxidase were exposed to 0.025% DAB (Sigma Chemical Company, St. Louis, MO) and 0.016% hydrogen peroxide (Fisher Scientific, Pittsburgh, PA) in PBS for 10 min. After washing, 10 sections of the spinal cord of each animal were put on glass slides, dehydrated in series of ethanol, cleared in xylene, mounted in Permount, coverslipped and examined in a Nikon Optiphot light microscope.

2.5. Histological evaluation and statistical analysis

The sections were examined for both the number of neurons and the percentage of PARP-staining neurons. All pyramidal neurons were counted in 5 randomly selected areas of layers III and V of the motor cortex of the SALS and control patients using a 125× magnification. Cells with positive (dark-brown, or black) nuclear staining for

PARP were counted in the same fields. In the parietal cortex, the large neurons were counted regardless of their shape. In the same area, the neurons immunostained for PARP were also counted. In the sections of the cerebellum, the Purkinje cells were counted in 5 randomly selected areas; the immunostained cells were then counted as well. The numbers of immunostained neurons from each individual patient were pooled and expressed as a percentage of the total number of cells counted. The density of PARP-positive glial cells and macrophages in the subcortical white matter in the motor cortex, parietal cortex and cerebellum was also determined, using the digital image analysis system (Optimas 6.2; Optimas Corp., Bothell, WA). The average density of subcortical immunopositive cells in the motor area of the control tissues was arbitrarily chosen to be 100%. All of the measured densities in the subcortical white matter of the motor area of SALS and AD brains were compared with these values. Similarly, the average measured density of immunostained glial cells in the parietal and cerebellar subcortical white matter of the control patients was arbitrarily selected to be 100%. The densities of the immunostained glial cells in the parietal and cerebellar white matter of the SALS patients and normal controls were expressed in comparison with this value, as percentages. All values for the results of immunoblots in the Figures and the text are expressed as means (± standard error). The total numbers of pigmented (neuromelanin-containing) neuronal cell profiles and immunostained profiles (cell nuclei for PARP and NF-κB, cytoplasm for parvalbumin) were counted in the whole cross-sections of the SN. As the neuronal cell content was different in the different cases (very low in PD and DLBD), the numbers of immunostained neurons were expressed as percentages of the number of all neurons containing pigment. The data were analyzed statistically with ANOVA (Excel software).

2.6. Western blot analysis

PARP-imunoreactivity (PARP-IR) was determined by immunoblot analysis. Samples to be analyzed were taken from the frozen brain specimens by separating small pieces (approximately 0.5 g) from the motor cortex, parietal cortex and cerebellum without thawing the tissue. Samples were homogenized with Wheatman homogenizer on ice in 20 mM HEPES buffer (pH 7.6, containing 200 mM KCl, 2 mM EGTA, 2 mM EDTA, 10 mM sodium molybdate, 50 mM sodium fluoride, 2 mM sodium pyrophosphate, 1

mM sodium vanadate, 0.1% NP-40, 10% glycerol, 4 mM benzamidine, 15 μg/ml aprotinin, 50 μM leupeptin, 1 μM pepstatin, and 1 mM phenyl-methyl-sulfonyl fluoride). The homogenized samples were sonicated twice with Sonic 300 Dismembrator (Artek, Farmingdale, NY) for 20 s. Protein content was measured by the Bradford method (BioRad, Hercules, CA). Each well was loaded with 100 mg of total protein from SALS and control patients. Protein samples were subjected to 8% sodium dodecyl sulfate polyacrylamide gel electrophoresis (SDS-PAGE) and transferred to nitrocellulose membranes by electroblotting. The nitrocellulose membranes were blocked for 2 h at room temperature with 5% powdered milk in PBS containing 0.05% Tween-20, then probed for PARP using the purified mouse anti-human PARP monoclonal antibody 7D3-6 (Pharmingen, San Diego, CA) at a 1:1000 dilution. The membranes were processed by using a horseradish peroxidase-conjugated anti-mouse secondary antibody, and the signals were detected by using ECL chemiluminescence (Amersham Pharmacia, Piscataway, NJ). The reliability of sample loading and electroblotting in each experiment was evaluated by stripping the membranes (Reprobe, Geno Technology Inc., St Louis, MO) and reprobing the blots with an antibody to actin (A4700; Sigma, St Louis, MO). Densitometric analyses were conducted with Image-J software (NIH image systems).

12.7. Electron microscopic techniques

For electron microscopic immunohistochemistry, the remaining sections (labeled with peroxidase or ferritin) were postfixed in 2.5% glutaraldehyde and 7.5% sucrose containing 0.1 M sodium phosphate buffer for 2 h at 4 °C. They were then contrasted in 1% uranyl acetate for 30 min, dehydrated in an ethanol series and embedded in Spurr (Electron Microscopy Sciences, Forth Washington, PA). Semi-thin sections (500 nm) were cut with an RMC-MT-7 ultramicrotome, and stained with heated 1% toluidine blue on glass slides. The regions of the MNs were identified under a light microscope, and from these areas 70-nm thin sections were prepared. From both group of samples (labeled with peroxidase or with ferritin) put on grids, every other section was contrasted with 7.5% magnesium uranyl acetate for 6 min and 3% lead citrate for 3 min. The contrasted and noncontrasted sections were examined in a CM-12 Philips electron microscope. Images of interest were recorded with a Gatan camera attached to the

electron microscope and stored in a computer for morphometric analyses with Optimas software (Bioscan Inc., Edmonds, WA). Three noninjected mice were also examined with the same methods.

From each mouse (15 inoculated with ALS IgG and 15 injected with control IgG), 17-25 neuromuscular junctions were examined to attain a total area of 25 μm^2 for both peroxidase and ferritin-labeled sections at a magnification of 20000x. For quantification of the IgG content of the ATs, ferritin-labeled ultrastructural sections were used. The areas of the ATs were determined via the software program and all of the ferritin granules were counted. The densities of the granules were expressed in terms of the mean number of molecules/μm^2 characteristic for each animal, for each group of animals that received the same IgG sample (n=3), the group of animals that received ALS IgG samples (n=15) and the group injected with the control IgG (n=15).

All the original numerical data were analyzed statistically with two-way repeated ANOVA with one between-subjects effect (the group of animals injected with ALS IgG versus the control group) and one within-subjects effect (densities of ferritin granules in axon terminals (ATs)). Ten large MNs in the ventral horns of the spinal cord of every mouse (approximately 400-600 μm^2 area for each) were evaluated similarly to the motor ATs. The areas of the rough endoplasmic reticulum (RER) were determined with the software program and the ferritin granules were counted and expressed as mean densities/μm^2. The statistical evaluation was performed in the same way as above. Five large MNs in the ventral horns of the spinal cords of the human samples (approximately 3000-4000 μm^2 for each) were evaluated similarly to the mouse MNs. The areas of the RER were determined with the software program, while the ferritin granules were counted. The density of ferritin bound to molecules of human IgG was expressed as the number of molecules/μm^2. Two-way repeated ANOVA with one between-subjects effect (the group of ALS spinal cords versus the group of control spinal cords) and one within-subjects effect (the density of ferritin granules in the RER of individual cells) were used for statistical evaluation. The amount of IgG represented by ferritin molecules and presumably bound to microtubules and located in the lysosomes, or in the multivesicular bodies in the endothelial cells, was not analyzed quantitatively.

3. Results

3.1. PARP expression in different brain regions of patients with SALS (paper 1)

We have found that PARP-IR was increased in the SALS motor cortex, parietal cortex and cerebellum as compared with the controls, as exemplified by a representative immunoblot (Fig. 1).

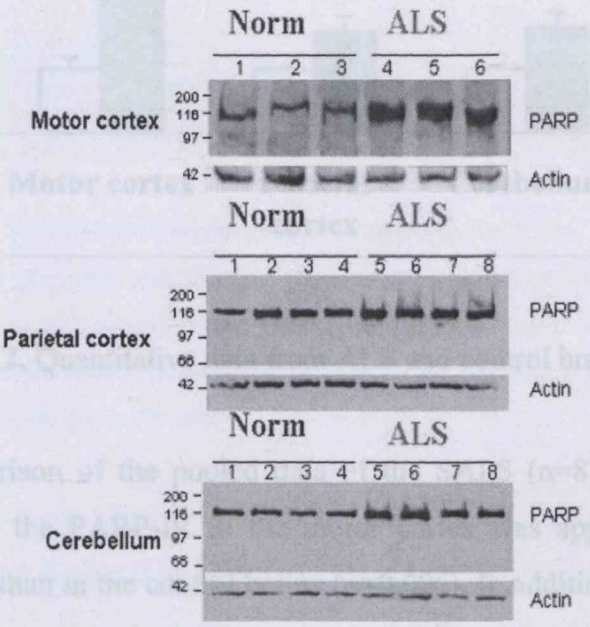

FIG. 1. PARP immunoreactivity in different regions of ALS and control brains. The representative enhanced chemiluminescence photographs of immunoblots demonstrate increased PARP-IR in homogenates of the motor cortex, parietal cortex and cerebellum as compared with the control (Norm). Each well was loaded with 100 μg of total protein, and blots were probed with anti-PARP monoclonal antibody. The membranes were stripped and reprobed with an anti-actin antibody as an internal control.

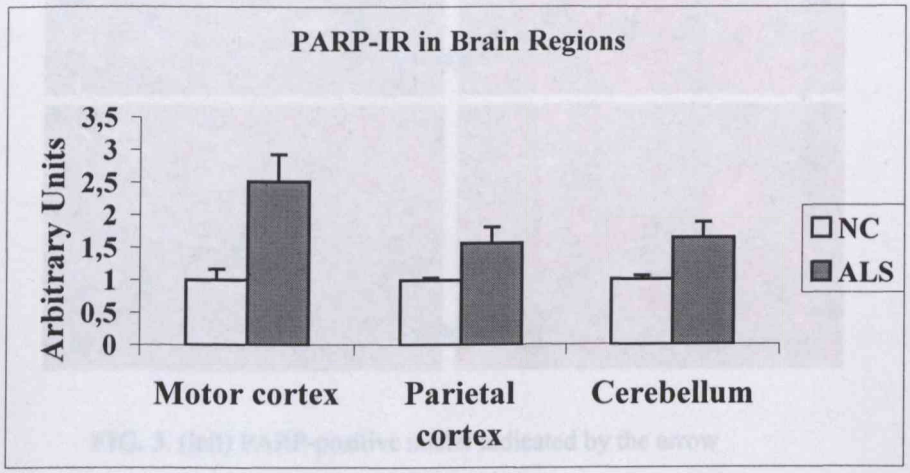

FIG. 2. Quantitative data from ALS and control brains.

Quantitative comparison of the pooled data of the SALS (n=8) and normal controls (n=4) revealed that the PARP-IR in the motor cortex was approximately 2.5 times higher in the SALS than in the control brains (p=0.006). In addition, the levels of PARP in the parietal cortex and cerebellum were each about 1.6 times higher than that in the normal controls (FIG. 2).

3.1.1. PARP in the motor cortex

While the normal neuronal density was preserved in the motor cortex in both the AD and the two normal control sections, the number of pyramidal cells was decreased in the SALS motor cortex, and especially the numbers of gigantocellular pyramidal cells in layers V and III (FIG. 3). One of the SALS patients had one-third of the number of neurons and the second had one-quarter of the number of neurons in the control patients. Most of the remaining pyramidal cells in the SALS motor cortex expressed strong dark-brown or black nuclear staining, leaving the nucleolus unstained.

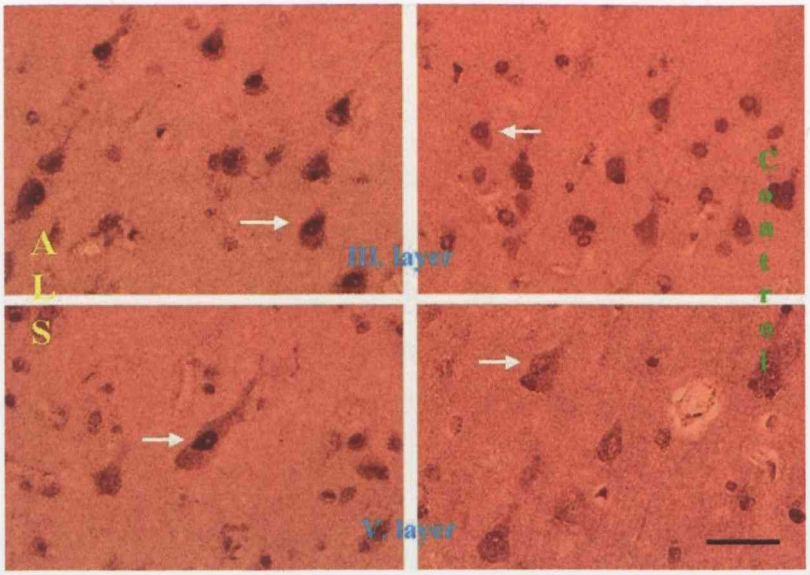

FIG. 3. (left) PARP-positive nuclei indicated by the arrow in the pyramidal cells in layers III and V of the motor cortex from an ALS patient. (right) There is no PARP staining in the pyramidal cells in layers III and V from the normal control. The scale bar is 100 μm.

The percentage of neurons immunostained and the overall intensity for PARP in the ALS motor cortex were higher than in the control or AD tissue (Fig.4).

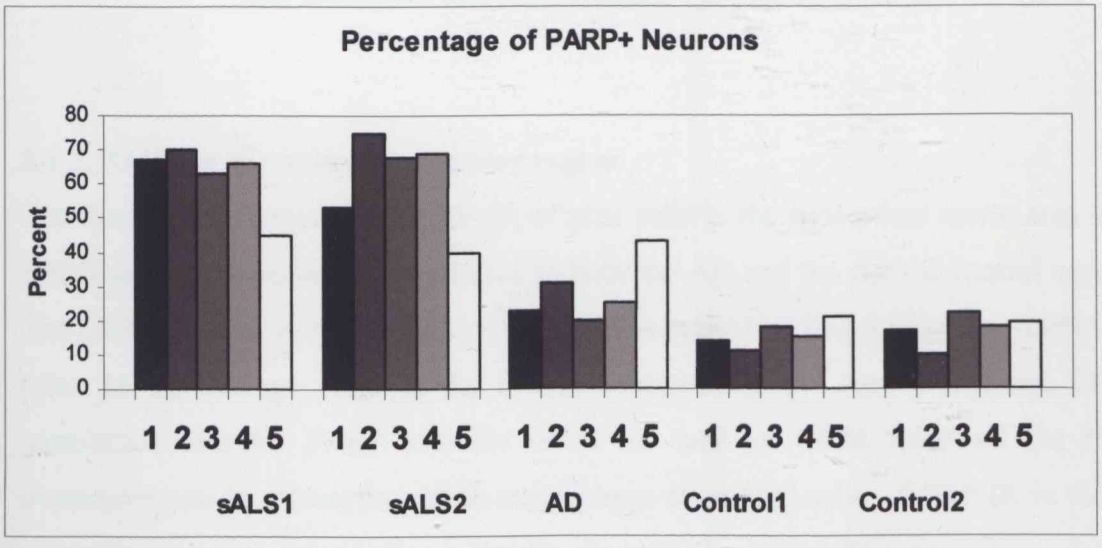

FIG. 4. The percentage of PARP-positive cells was increased in the ALS sections as compared with the control and ALZ (Alzheimer) sections. 1 = neurons in layer III of the motor cortex; 2 = neurons in layer V of the motor cortex; 3 = neurons in layer III of the parietal cortex; 4 = neurons in layer V of the parietal cortex; 5 = Purkinje cells in the cerebellum.

3.1.2. PARP in the parietal cortex

The parietal lobes were also examined. While there was no decrease in the number of neurons in the parietal lobe of the SALS brains, the number of PARP-immunostained neurons in the parietal cortex was increased relative to the AD and normal controls, similarly to the increase seen in the motor cortex. The staining in the AD parietal cortical sections was similar to that in the normal controls (Fig. 5).

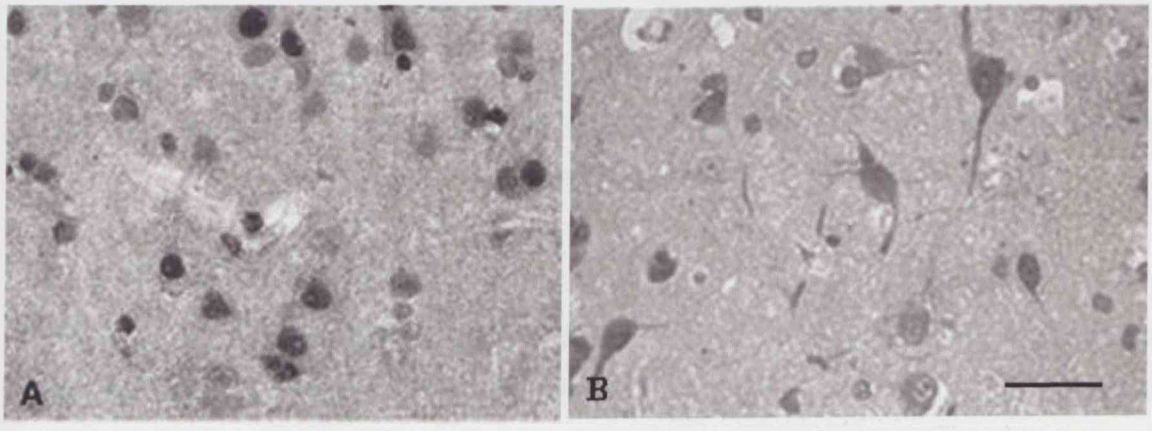

FIG. 5. PARP-immunopositive neurons in the parietal cortex in a patient with ALS as compared with a control patient. The scale bar is 100 μm.

3.1.3. PARP in the subcortical motor region

The density and intensity of PARP-IR of glial cells in the subcortical motor area in the SALS sections were increased relative to both the AD and the normal control sections. The PARP-IR was increased by 515% and 482% in the two SALS samples, 100% being taken as the average value in the frontal subcortex of the control sections. Double immunostaining for PARP and for GFAP as well as CD68 localized the PARP overexpression to astrocytes and to macrophage-microglial cells. PARP-IR in the AD subcortical sections was similar to that for the control sections (FIG. 6).

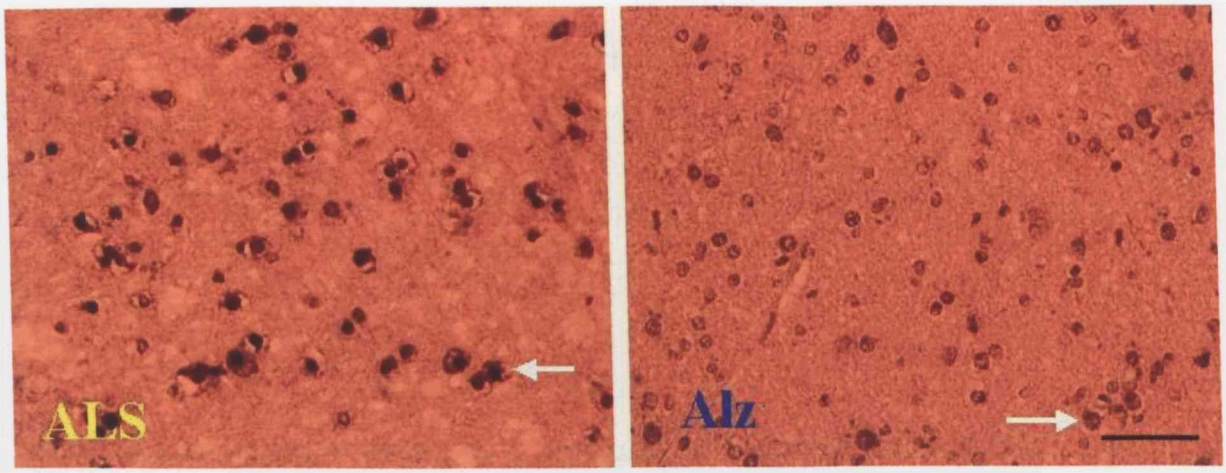

FIG. 6. The dark nuclei of subcortical glial cells indicated by the arrow in the frontal region of the ALS brain express strong PARP immunostaining as compared with a patient with Alzheimer disease. The scale bar is 100 μm.

3.1.4. PARP in the cerebellum

While there was no decrease in the number of Purkinje cells in the cerebellum in the SALS or AD, the intensity of PARP for the two SALS sections and the AD sections was increased as compared with the controls. In addition to the Purkinje cells, the cells of the granular layer displayed stronger immunostaining in SALS tissues than in the AD or normal control tissues (FIG. 7). The cerebellar granular cells from the AD also exhibited a stronger immunostaining than that in the normal controls.

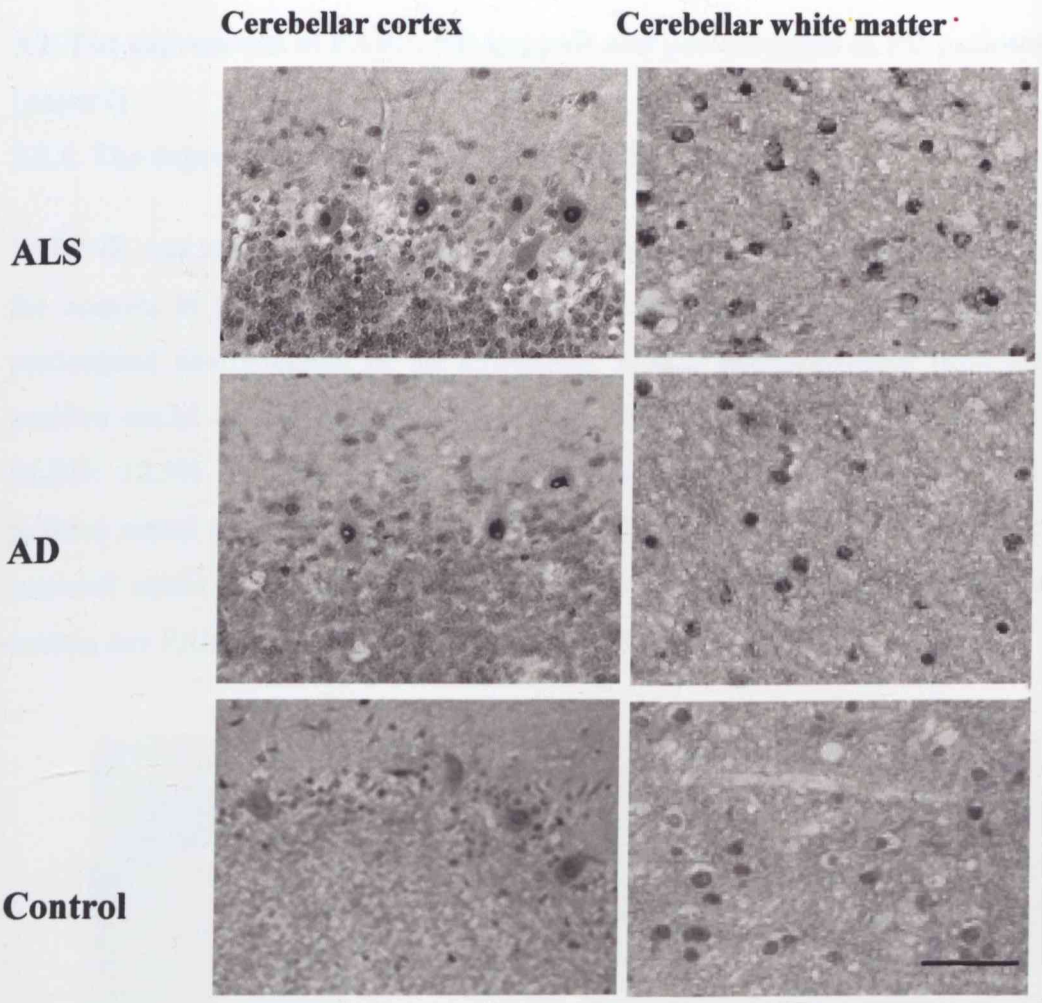

FIG. 7. (left) The nuclei of the Purkinje cells in the cerebellum of an ALS patient are strongly immunostained for PARP. Strong immunostaining of the nuclei of Purkinje cells for PARP in the cerebellum of an AD patient. The nuclei of the Purkinje cells are slightly immunostained for PARP in a normal control cerebellum. (right) The nuclei of glial cells in the cerebellar white matter of an ALS patient express moderate immunostaining for PARP. There is also a moderate staining in the glial cells from an AD patient. The immunostaining for PARP is lighter in the glial cells of the white matter of a control cerebellum. The scale bar is 100 μm.

The densities of the PARP positive cerebellar glial cells in the white matter were also a little higher in the SALS tissues as compared with the control tissues (157% and 151% increased, 100% being the average value in the cerebellum of the control tissues). The subcortical cerebellar glial cells stained a little more intensely in the AD sections than in the normal controls (121% increased).

3.2. The expressions of PARP, NF-kappaB and parvalbumin in PD patients (paper2)

3.2.1. The expression of PARP in the SN in PD

PARP-IR was noted as a dark-gray peroxidase reaction product confined to the nuclei of the neurons in the SN in PD and DLBD. Most of the neurons contained dark-brown particulated neuromelanin in the cytoplasm, readily distinguishable from the PARP-positive nuclei by its shape and color (Fig. 8a). In the SN of samples from PD and DLBD, 12.5% to 40% of the neuromelanin-containing neurons displayed PARP-positive nuclei (Fig. 12). Only one of the AD brains contained PARP-immunopositive neuronal nuclei in the SN, and only in 8% of the cells. Other control samples did not contain any PARP-immunopositive neurons in the SN (Fig. 8b).

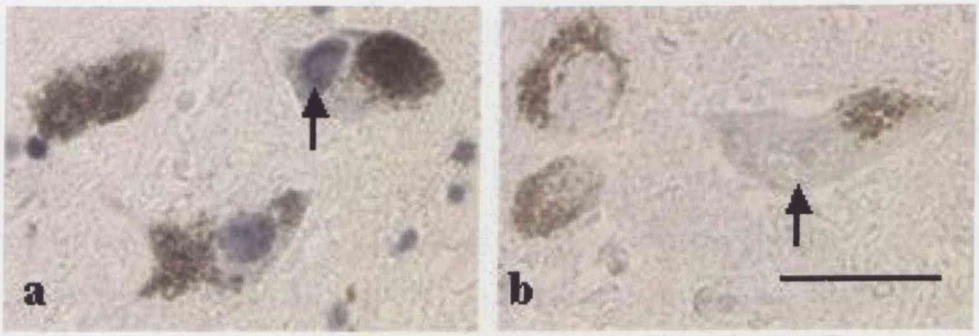

FIG. 8. (a) Expression of PARP as a dark-gray peroxidase reaction product in the DA-ergic cells in the SN of a PD patient (arrow). (b) There is no PARP staining with the same immunohistochemical reaction in the nucleus of the DA-ergic cells in the SN from a control sample (arrow). The scale bar is 70 μm.

The difference between the PD + DLBD group and the control group was statistically highly significant ($p < 0.0002$). The nuclei of many of the glial cells were also immunostained positively, but they were not further identified as astrocytes, oligodendrocytes or microglial cells.

3.2.2. The expression of parvalbumin in the SN in PD

Immunostaining for parvalbumin revealed that 16% to 42% of the neurons in the SN of the patients with PD and DLBD contained cytoplasmic parvalbumin colored brown by the non-metal-enhanced DAB and distinct from the blue-black neuromelanin counterstained with hematoxylin (Fig. 9a, b).

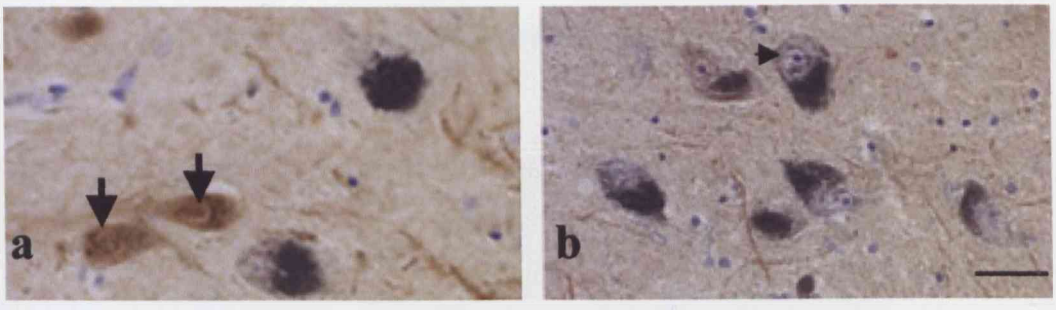

FIG. 9. (a) Parvalbumin in the cytoplasm of the dopaminergic cells in the SN from a PD patient. One of the cells is indicated by arrows. There is no staining for parvalbumin in the cells in the control SN (arrowhead) (**b**). The scale bar is 70 μm.

In the control samples, 3.2% to 14% of the neurons in the SN exhibited an immunopositive parvalbumin content (Fig. 12). The difference between the two groups was statistically significant ($p < 0.00004$). Double immunostaining for PARP and parvalbumin proved that none of the parvalbumin-containing neurons displayed increased PARP staining in the nucleus, and none of the PARP-immunopositive neurons displayed parvalbumin reactivity in their cytoplasm.

3.2.3. The expression of NF-κB in the SN in PD

Nuclear translocation of the NF-κB were seen in the SN patients with PD and DLBD (FIG.10b). The translocation of NF-κB from the cytoplasm to the nucleus occurred in 6% to 31% of the neurons in the SN in the group of PD and DLBD. Two of the AD cases exhibited a similar translocation of the NF-κB in 4% and 7% of the neurons (FIG. 12). In the other control cases, the translocation occurred in less than 1% of the cells (FIG.10a). The difference between the two groups was statistically highly significant ($p < 0.0006$).

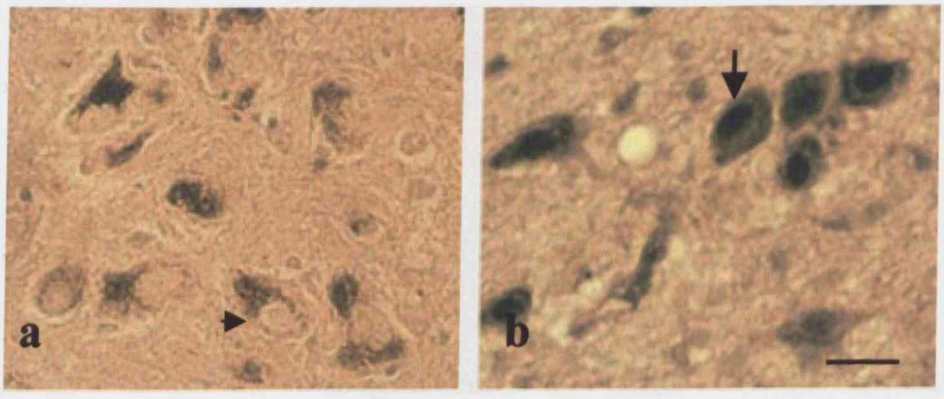

FIG. 10. NF-κB-positive nuclei **(b)** (arrow) in DA-ergic cells of the SN from a patient with PD. There is no immunoreactivity for NF-κB in the control sample (arrowhead) **(a)**. The scale bar is 70 μm.

3.2.4. Colocalization of PARP and NF-κB

Consecutive sections immunostained for PARP (Fig. 11a) and for NF-κB (Fig. 11b) proved that, in all of the neurons which exhibited translocation of NF-κB in the nucleus, PARP was also upregulated. However, the number of neurons with upregulated PARP was a little higher in every case than the number of cells involving the translocation of NF-κB.

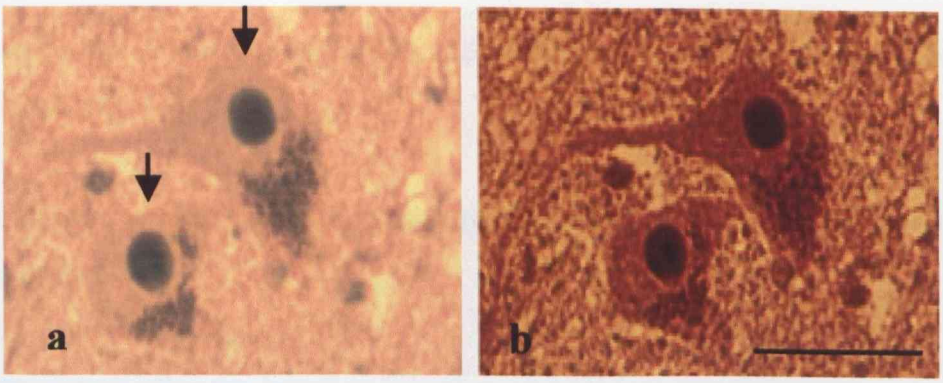

FIG.11. (a) PARP expression in the nuclei of DA-ergic cells in the SN from a PD patient. The peroxidase reaction product is dark-gray (arrows). (b) Strong NF-κB immunostaining in the nuclei of the same cells in a consecutive section. The peroxidase reaction was developed with VIP substrate reagent. The scale bar is 70 μm.

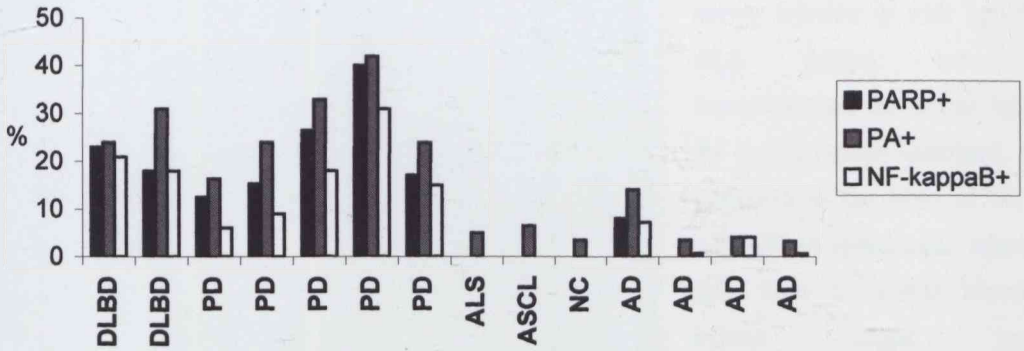

FIG. 12. The percentages of DA-ergic cells in the SN expressing PARP-IR (black-columns), with nuclear translocation of NF-κB (white columns) and parvalbumin–IR (striped columns). PD: Parkinson disease. DLBD: diffuse Lewy body disease, ALS: amyotrophic lateral sclerosis, AD: Alzheimer disease, ASCL: generalized atherosclerosis, NC: normal control.

The DA-ergic cells of the SN in DLBD and in PD patients contained significantly higher proportions of immunostained cells for all three antigens than the SN from control tissues. Only one AD case expressed all three antigens, but in much lower proportion than the average in PD. The nuclear translocation of NF-κB staining and PARP-IR revealed a significant overlap in the neurons, while the immunostaining for

parvalbumin did not overlap with the cells reactive for the previous two examined antigens (Fig. 12).

3.3. Appearance of human IgG in spinal MNs of mice following ip inoculation (paper 3)

3.3.1. Detection of IgG in MNs

Forty-eight h after the initial ip injection of ALS IgG, the IgG immunoreactivity could be detected by the light microscopic immunohistochemical method in the perikarya of the spinal MNs of mice as a dense, dark peroxidase reaction product, leaving the nuclei unstained. All 5 ALS IgG samples gave similar reactions in all of the mice injected. The control samples gave much lighter uniform reactivity in the perikarya of the MNs of the mice injected similarly with the same dose of IgG (Fig. 13 A,B).

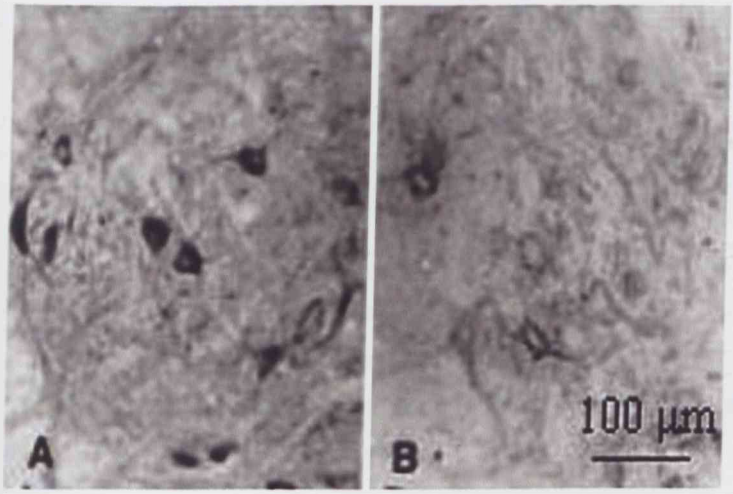

Fig. 13. (A) The perikarya of MNs of the ventral horn of the spinal cord of a mouse injected ip with IgG from an ALS patient are heavily immunostained for human IgG, while the nuclei remain unstained. (B) The perikarya of the MNs of the ventral horn of the spinal cord injected with IgG from a normal blood donor exhibit slight peripheral immunostaining for human IgG.

No peroxidase reaction product was revealed in the spinal MNs of noninjected mice with the same detection system. When the detecting antibody (biotinylated) was omitted from the reaction, no immunostaining was noted in any of the examined MNs of the animals.

3.3.2. Human IgG detected in the RER of spinal MN of mice

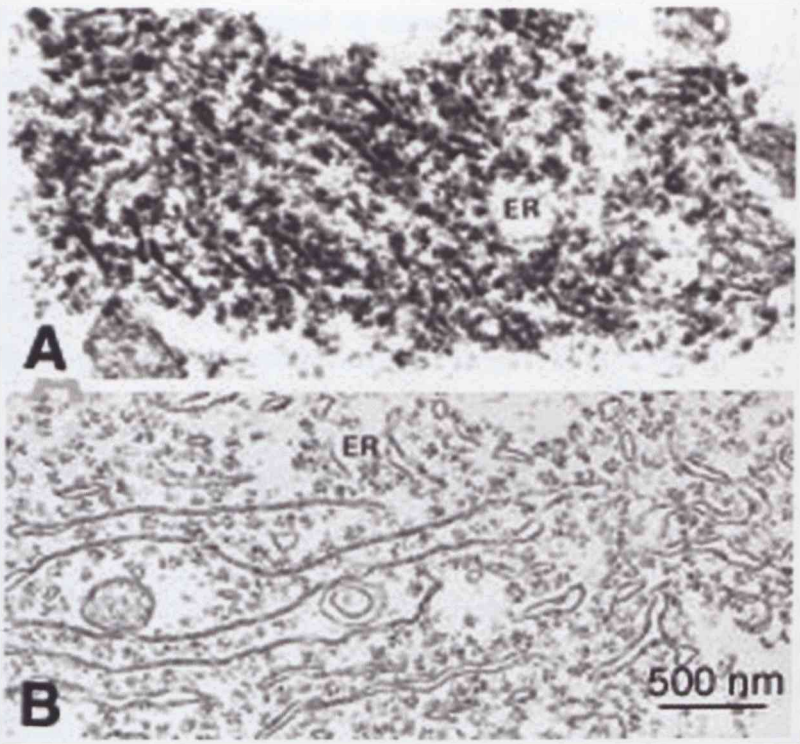

FIG. 14. The RER in a spinal MN from a mouse inoculated ip with IgG from an ALS patient is darkened and thickened by the reaction product of peroxidase, indicative of the human IgG content (A) as compared withthe normal appearance of the RER of the spinal cord from a mouse injected with normal human IgG.

The immunoreactivity of the ALS IgG was localized to the RER as precipitated peroxidase reaction product throughout the whole organelle. Both the membranes of the cisterns and the ribosomes were heavily labeled in all of the examined MNs (Fig. 14A). The RER in the MNs of the mice injected with the control IgG samples was not labeled at all, which was indicative that little or no IgG was taken up (Fig. 14B).

The detection of human IgG with ferritin-conjugated antibody allowed a quantitative comparison of the accumulation of the ALS IgG in the RER with the accumulation of the control IgG. In the RER of the MNs of the mice injected with the ALS IgG, the density of ferritin granules was 154 ± 34 (SD)/μm^2 (n=50), while in the RER of the MNs of the mice injected with the control IgG it was 7 ± 3 (SD)/μm^2 (n=50). The

difference between the two groups is highly significant statistically ($p < 0.0001$, $F = 109.469$).

3.3.3. IgG detected localized to microtubules of the MNs

Microtubules were identified as other structures labeled specifically with ferritin-conjugated anti-human IgG in the perikarya and in the axons of the spinal MNs of the mice inoculated with the IgG from the ALS patients. In the cell body and in the dendrites, groups of ferritin molecules (8-12) were noted in the vicinity of microtubules distributed randomly (not at equal distances from each other). In the peripheral axons, mostly single molecules were arranged in lines (Fig. 15A,B).

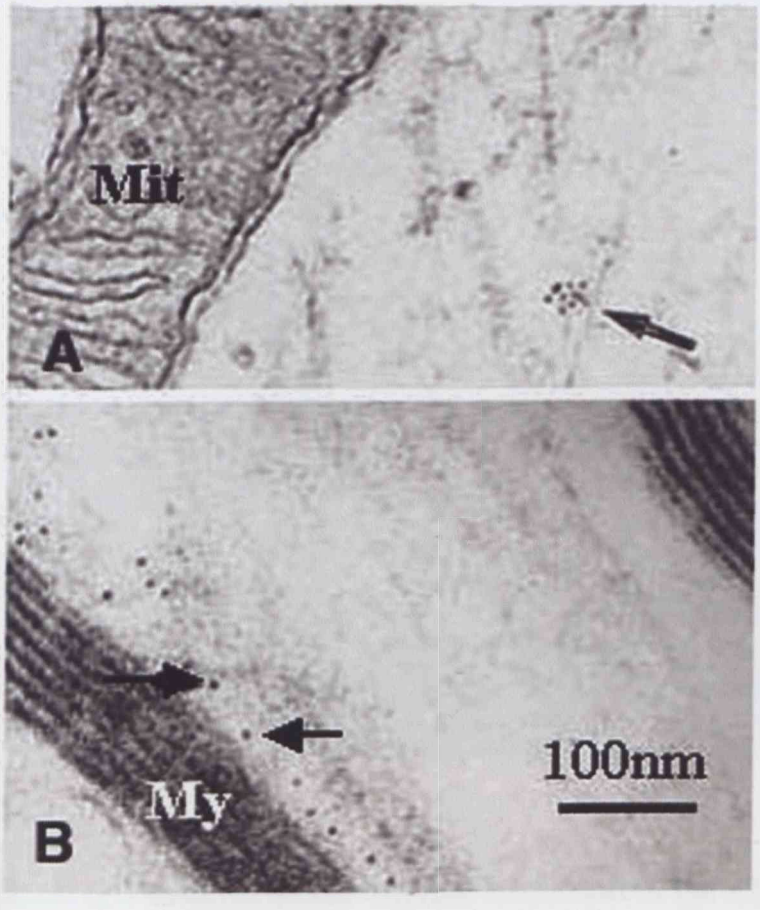

FIG.15. (A) The ferritin-labeled antibody localizes IgG to a microtubule in the dendrite of a spinal MN (arrow) of a mouse injected ip with ALS IgG. **(B)** Human IgG is localized by ferritin molecules (arrows) to the periphery of a motor axon in the interosseous muscle of a mouse injected ip with ALS IgG. My: myelin, MIT: mitochondrion

3.3.4. The detection of IgG on the external surface of a Schwann cell

At the neuromuscular junctions of the mice, the ALS IgG and the control human IgG was bound heavily to the external surface of the Schwann cells as detected with

peroxidase-labeled antibody. While the IgG from the ALS patients seemed to induce its own endocytotic uptake as IgG-containing omega formations (invaginations) from the cell membrane (Fig. 16 a,b), the control IgG samples remained on the surface (Fig. 16 c).

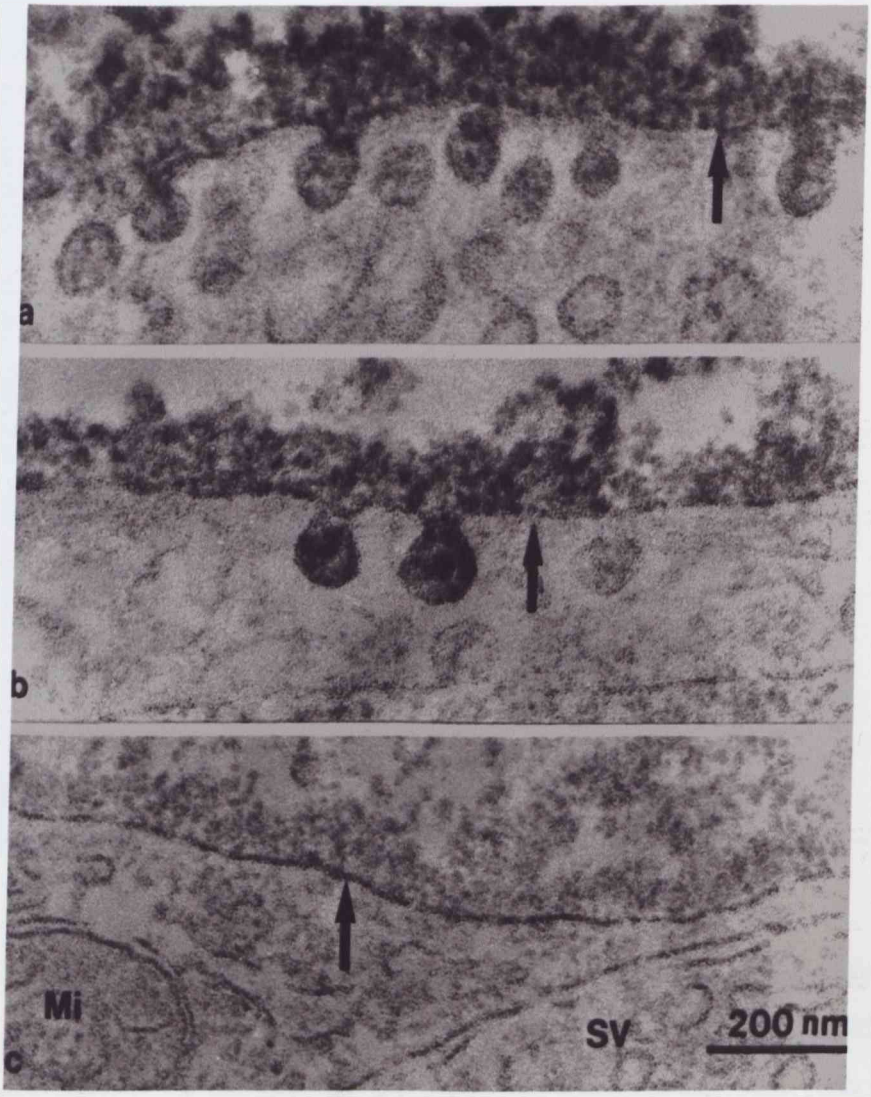

FIG.16. (a,b) IgG labeled with the reaction product of peroxidase conjugated to the detecting antibody on the surface of a Schwann cell (arrows) at the neuromuscular junction of a mouse injected with ALS IgG. The IgG is taken up in vesicles displaying omega formations. **(c)** Normal human IgG (arrow) does not induce its own uptake on the surface of the Schwann cell in the mouse injected with normal control IgG. Mi: mitochondrion. SV: synaptic vesicles.

3.3.5. IgG detected on the external membrane of the AT

The attachment of IgG to the external membrane of the ATs as a possible uptake site could not be visualized in any of the ATs examined. Nevertheless, the IgG from the ALS patients that was taken up in the motor ATs could be identified with the ferritin-labeled antibody. The ferritin granules were located in synaptic vesicles and attached to their external surface (Fig. 17A, B).

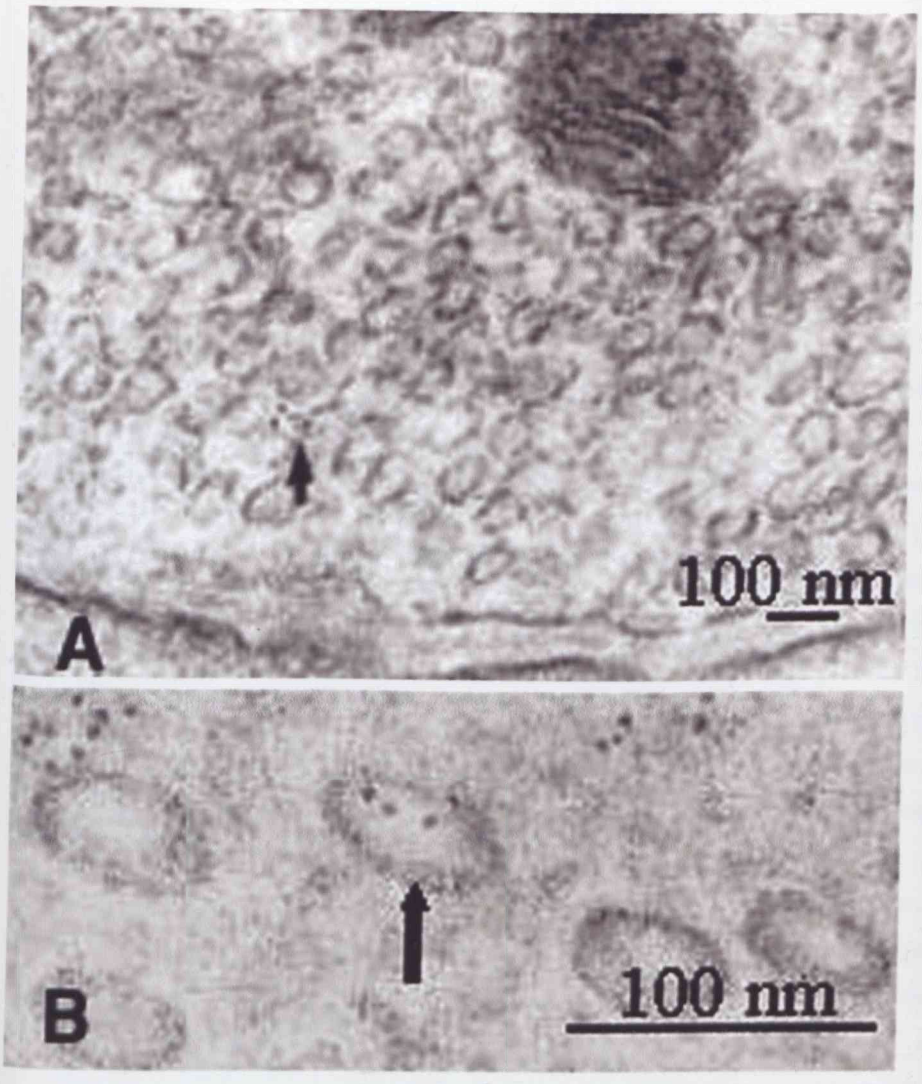

FIG. 17. (A) IgG detected with ferritin-labeled antibody in the motor axon terminal of a mouse injected ip with IgG from an ALS patient (arrow). **(B)** The ferritin molecules localize the IgG within the synaptic vesicles (arrow), or attached externally to their membrane.

The localization and the abundance of the ferritin granules identifying IgG in the motor ATs seemed to be specific for ALS IgG, because ferritin labeling was found only accidentally in the ATs of the LMNs of the mice injected with the same amount of control IgG. In the ATs of the spinal MNs, the mean density of ferritin granules was 37 ± 3.36 (SD)/μm^2), which was considerably higher than the mean density in the motor ATs of the mice inoculated with the control IgG (3.8 ± 2.14 (SD)/μm^2). The difference between the two groups was highly significant statistically ($p < 0.0001$, $F = 561.73$).

3.3.6. IgG detected in the EC in mice and in patients with ALS

About two-thirds (51 of 75) of the endothelial cells (ECs) in the ventral horns of the spinal cords of the mice inoculated with the ALS IgG contained 2-3 multivesicular

bodies filled with IgG in the cytoplasm, as detected with peroxidase or ferritin-conjugated antibodies (Fig. 18A). In the control IgG-injected animals, multivesicular bodies were observed in only about one-tenth of the endothelial cells (8 of 75).

Ultrastructural localization of IgG in spinal MNs of ALS autopsy material.

In the human autopsy material, the ultrastructure was severely compromised by the *post mortem* autolysis.

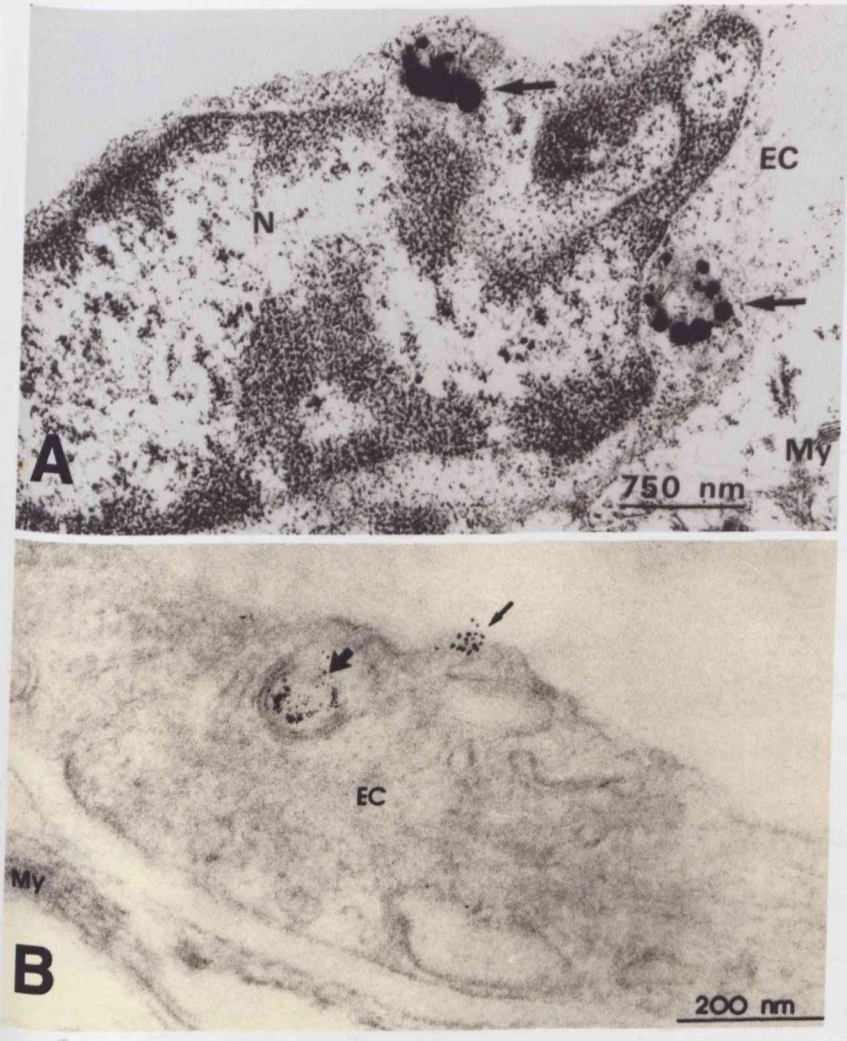

FIG. 18. (A) The peroxidase reaction product labels human IgG in multivesicular bodies (arrows) in the endothelial cell (EC) in the ventral horn of the spinal cord of a mouse injected ip with ALS IgG.

(B) IgG labeled with ferritin-conjugated antibody is taken up in an EC in the ventral horn of the spinal cord of a patient who died from ALS. The ultrastructure is severely compromised by the postmortem autolysis, but the IgG can be localized to a multivesicular body (thick arrow). The thin arrow indicates IgG molecules attached to the surface of the cell. My: myelin; N: nucleus; EC: endothelial cell

One or two multivesicular bodies filled with IgG were detected with ferritin- labeled antibody in almost one-third (9 of 30) of the examined ECs in the ventral horns of the ALS spinal cords (Fig. 18B), but none in the control tissues. There were traces of IgG on the surface of the ECs in tissues from the ALS cases and from the controls.

3.3.7. IgG detected in proximity to microtubules and in the RER in patients with ALS

IgG could be detected with ferritin-labeled antibody in the spinal MNs of the ALS patients. Ferritin molecules were localized to the RER in large groups (containing 30-50 molecules) and to the microtubules in smaller groups (6-14 molecules).

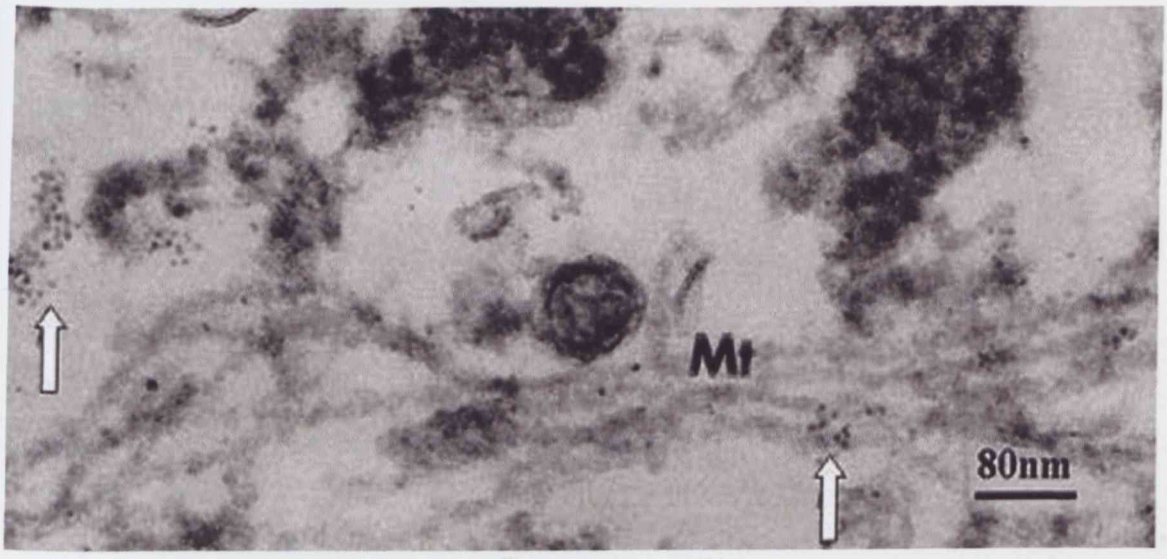

FIG. 19. In spite of the severely compromised ultrastructure, the IgG can be localized to the RER (left arrow) and to the microtubules (Mt) (right arrow).

The density of the ferritin molecules was calculated to be 271 ± 43 (SD)/μm^2 (n=25) in the RER in the spinal MNs of the ALS samples and 9 ± 4 (SD)/μm^2 (n=25) in the RER of the control tissues. The difference between the two groups was highly significant statistically ($p \leq 0.0001$, $F = 1053.45$).

The interactions were not significant in the data obtained from the groups (MNs of mice: $p = 0.205$, $F = 1.754$; ATs in mice: $F = 0.839$, $p = 0.45$; MNs in human spinal cords: $F = 1.655$, $p = 0.185$).

4. Discussion

In the UMNs, there is an overactivation of PARP. This overactivation could lead to the excessive consumption of NAD^+ and the depletion of internal energy sources, further aggravating the ATP deficit (57) of the UMNs. The resulting energy failure could jeopardize the function of the ATP-requiring ionic pumps which maintain the electrochemical gradients across neuronal plasma membranes, leading to apoptosis (58) and/or necrosis (59) of the UMNs. Clearly, we can state that PARP overactivation may be responsible for the death of the UMNs in ALS. Thus, with respect to PARP-IR, the spinal MNs appear to behave in an opposite way to the pyramidal neurons, because there is an increase in the PARP level in the UMNs, and a decrease in the LMNs (60, 61). A potential explanation is that the spinal MNs may have evolved mechanisms to prioritize other highly ATP-dependent processes, such as ubiquitination and proteosomal removal of aggregated proteins (62), decreasing the intracellular Ca^{2+} level, enhancing the altered axoplasmic transport (63) and preserving neurotransmitter release from an increased number of sprouted axon terminals in ALS. The death of the LMNs may occur because of the functional deficiency of the enzyme for repair of the injured DNA. Further studies are required to explain the differences in PARP reactivity in the UMNs and LMNs. This type of abnormal activation of PARP has been implicated earlier in the development of cell damage in MPTP-induced PD (64), AD (65), ischemic brain damage (66) and CNS trauma (67).

The increased expression of PARP-IR was not confined to the motor cortex in ALS patients, but was also increased in the neurons of the parietal and cerebellar cortices, (though on less extensively) areas, which are not known to be involved in ALS pathogenesis.

The slight overactivation of PARP in other than motor areas may reflect the situation that oxidative stress is widespread in the ALS brain. As only MNs die selectively in ALS, we presume that the PARP overactivation only in these cells exceeds the threshold of being irreversibly damaging.

The significant increase in PARP expression in the nuclei of a subset of DA-ergic neurons in the SN in PD and DLBD may be a consequence of both oxidative damage and an increased intracellular Ca^{2+} level leading to apoptosis. PARP is required as coactivator for the nuclear translocation and transcriptional activation of NF-κB in DA-

ergic neurons. NF-κB has been implicated in the regulation of genes involved in many processes, including apoptosis. The molecular mechanism for the damage of the DA-ergic neurons in the SN in PD may be the transcriptional activation of oncogene p53, inducing programmed cell death (68, 69). The relevance of this mechanism in PD has been questioned by others (70) because NF-κB is protective in other neuronal cell types (71) and also in PC12 cells (72). The nuclear translocation of NF-κB was noted in cells which also expressed an increased PARP level, as evidenced by the immunostaining of consecutive sections for the two different antigens. The data support the view that NF-κB promotes apoptosis (73), because PARP can also serve as a marker for the onset of programmed cell death (74).

Besides the MNs, PARP is also increased in the microglia cells and astrocytes. PARP is necessary for the activation of microglia and macrophages. Following activation, the microglia and macrophages release free radicals (75, 76), which could damage the cell membrane of neighboring neurons and the astroglial glutamate transporter. Microglia can also enhance neuronal injury by releasing the cytokines IL-1β, IL-2, IL-6, IL-10, , TNF-α, IFN-γ (76, 78), iNOS, COX-2, glutamate (77), all of which could lead to a raised intracellular Ca^{2+} level in the neurons, increased neuronal free radicals and subsequent DNA damage and PARP activation. The soluble constituents released from the microglia could also diffuse widely from their release sites. This can be the explanation why other than MNs express increased PARP in ALS.

PARP-IR is also increased in the astrocytes. Since the astroglia may be an important source of antioxidant protection (79-81) and releases neurotrophic factors, the increased PARP-IR in the astrocytes indicates a somewhat compromised ability to mediate critical neuroprotective functions (82, 83).

PARP-IR is also increased in the neurons in the parietal and cerebellar cortices, areas which are not known to be involved in ALS pathogenesis. This means that in ALS there is a widespread oxidative stress in the CNS. The fact that parietal neurons express increased PARP in ALS, yet do not degenerate, could be a reflection of their increased resistance to the toxic effects of the "stressor(s)." If, as proposed, oxidative stress is the major "stressor", then increased intracellular Ca^{2+} could result from the increased oxidative stress. The relative resistance of the parietal cells could relate to their ability to buffer the increased Ca^{2+} load due to the ample presence of the Ca^{2+}-binding proteins

calbindinD28K and/or parvalbumin. Furthermore, non-MNs, such as parietal lobe neurons, may well have more efficient antioxidant capacities than MNs. The Purkinje cells in the cerebellum appeared to be partially protected from PARP increases, possibly because of their well-known high concentrations of the Ca^{2+}-binding proteins calbindinD28k and/or parvalbumin (84).

Increased oxidative stress (85-94) provides a potential explanation as the general cause of the neuron damage, but the source of such enhanced oxidative stress is unknown. The presence of widespread microgliosis is a potential clue. Alternatively, the enhanced microgliosis could be a response to increased oxidative stress. However, our present data cannot differentiate oxidative stress that initiates microglial activation from oxidative stress that results from microglial activation. As microglia activation is dependent on PARP activation, and the microglia regulates the local immune-inflammatory response, the inhibition of PARP can decrease the immune/inflammatory processes. Meanwhile, the PARP inhibitors in neurons can save the cells from unnecessary energy depletion.

Furthermore, the increased number of astrocytes containing high amounts of PARP mainly in the motor cortex suggests that cells other than neurons may be subjected to pathologic stressors in ALS, and in turn, such altered glia may contribute to the pathogenesis of ALS.

Nevertheless, it is clear that the increased PARP-IR is not confined to the motor system, but is increased throughout many regions of the CNS of ALS patients, with the relative neuronal damage mediated by selective mechanisms of vulnerability and resistance. There is evidence that in SALS immune/inflammatory mechanisms are involved in the pathomechanisms of the disease. The anti-MN IgG is part of this process.

The effects of ALS IgG on the neurons vary under different experimental conditions, from cell destruction in cultures (95, 96), to the initiation of degeneration in vivo (97) and the increase of neurotransmitter release in vivo (28, 98) and in vitro (99). The changes seem to be mediated by the increase in the level of intracellular Ca^{2+} (100). The increase in intracellular Ca^{2+} is due to the effect of ALS IgG on the Ca^{2+} channels (101) and is promoted by Fcγ receptors (102). In our experiments, however, IgG bound to the external membrane of the motor Ats, where the Ca^{2+} channels are located, was not detected. One possible reason is the rapid uptake of IgG in the terminal. Nevertheless,

the demonstrated action of ALS IgG on the Ca^{2+} channels does not exclude the possibility that other subpopulations of IgG molecules exert their effects elsewhere in the cell.

The accumulation of IgG in the RER might interfere with the synthesis of proteins essential for the normal functioning of the MNs or induce an elevation of cytosolic Ca^{2+} due to release from the internal stores (103). However, the enrichment of IgG in the RER may also be fully secondary, due to a humoral immune response to the continuous release of antigens from previously destroyed MNs. They can be taken up passively by the internalization of synaptic vesicles from the plasma membrane of the ATs and find their antigen target intracellularly.

IgG bound to the microtubules in the cells may be of greater importance in inducing a cell dysfunction. Modifications of the proteins of the microtubules in ALS precede detectable ultrastructural changes in the axons (104). The microtubules determine the location and organization of the Golgi apparatus within the cells. Monoclonal antibodies directing to tubulin, a microtubule protein, lead to a dramatic dispersal of the Golgi apparatus when microinjected into cells (105). The fragmented neuronal Golgi is functional in ALS and in mice with the G93A mutation of the Cu/Zn SOD gene caused by the disruption of the microtubules (106). The significance of the alterations in the microtubules and fast axonal transport in inducing MN disease has been proved in Drosophila (107). Microtubules and NFs are linked by frequent crossbridges *in situ* (108), and the altered fast axonal transport can therefore compromise the slow transport too. The finding that ALS IgG is bound to microtubules in passive transfer experiments on mice and also in ALS tissue, and the above literature data demonstrating the significance of the dysfunction of the microtubules in MN disease, warrant further experimental work.

As ip administered ALS IgG raises the glutamate level in the CSF in rats, i.e. it acts on and can be detected in synaptic boutons residing on LMNs (109), it is envisaged that IgG accesses neurons from the extracellular space in the CNS. There is no proof of an overall disturbance of the blood-brain barrier functions in ALS, but our experiment yielded morphological evidence of the translocation or at least the uptake of IgG through CNS ECs in the affected areas of the spinal cord in ALS. There may be multiple antibodies targeting a variety of epitopes of MNs in ALS. Some of them have

been proved to be relevant in causing functional abnormalities, and even cell death in different cell cultures. IgG passively transferred from the sera of ALS patients to mice may be cytotoxic (110), or at least initiate the degeneration of MNs with ultrastructural alterations similar to those in the preliminary stages of apoptosis. The harmful effects of antibodies directed to antigens in the RER or bound to microtubules have yet to be proved.

The accumulation of IgG in MNs may serve only as signaling for the microglia and locally regulate the expression of complement receptors on it. Although the recruitment of microglial cells may be beneficial in to removing foreign materials, the sustained activity of these cells may have detrimental effects on the neurons (111).

The signs of chronic activation of the microglia and astrocytes occur in selected areas of damage in the CNS of patients with neurodegenerative disease such as SALS and PD.

In the passive transfer experiments, activated CD11b-positive microglial cells were demonstrated in the ventral horn of mouse spinal cords after the ip injection of IgG from SALS patients or from guinea pigs with experimental autoimmune gray matter disease. The latter is induced by the immunization of guinea pigs with the homogenate of the ventral horn of bovine spinal cord. The activated microglial cells can damage the neurons by releasing cytotoxic cytokines, excitatory neurotransmitters and ROS. Reactive microglia also releases the highly toxic peroxynitrite molecules, which inhibit the function of membrane proteins such as glutamate transporters located on the surface of the astrocytes, and in this way, they contribute to elevated glutamate levels and enhance excitotoxicity. The activated microglia may also have neuroprotective effects. It is known that microglial-derived IL-1 is required for the astrocytic production of ciliary neurotrophic factors and insulin-like growth factor 1, both of which help repair the damaged CNS. Thus, they can alter the phagocytic properties of the microglia and potentiate the engulfment of dying cells (112). From this point of view, the intracellular IgG is implicated in the local inflammatory process characteristic of ALS. As regards a low antibody level directed to certain MN antigens in the blood of ALS patients, as opposed to this, the enrichment, the undetermined length of stay and the effects of these multiple IgGs inside the MNs may contribute to the failure of immunosuppressive treatment (insufficient and too late) in ALS.

In vitro, the IgG of ALS patients binds to L-, N and P-type Ca^{2+} channels and enhances Ca^{2+} influx into cultured MNs (27). The increased intracellular Ca^{2+} activates PARP, which plays the already discussed important role in neuron degeneration. The enhanced PARP-IR could reflect enhanced activation of the DNA repair systems in response to widespread oxidative damage.

Oxidative stress (113), excitotoxicity (102) and immune/inflammatory (114, 115) processes act in concert in the pathomechanism of neurodegenerative diseases such as ALS and PD.

The common pathway of excitotoxicity, oxidative stress and inflammation involves increased level of intracellular Ca^{2+} in the damaged neurons. Our data indicate that the level of parvalbumin detected by immunohistochemistry is increased in the injured neurons in the SN in PD. We consider this to be an indirect sign of an increased intracellular Ca^{2+} level. There is no way to detect the *in vivo* Ca^{2+} content of the cells in autopsy material, because the *post mortem* autolysis influences the Ca^{2+} compartments in the cells. An increased parvalbumin level apparently helps the cell buffer an increased intracellular Ca^{2+} level. None of these neurons expressed an increased PARP level or the nuclear translocation of NF-κB as signs of an apoptotic process. It seems that a certain proportion of the neurons in the SN pars compacta upregulate parvalbumin in response to an increased intracellular Ca^{2+} level and, at least temporarily, are then protected from cell death, similarly to the neurons of the pars reticulata of the SN (116). The role of such an increase level of parvalbumin in protecting the MNs from death has been proved under experimental conditions (117, 118). The cells with increased PARP expression did not display a simultaneously increased parvalbumin immunoreactivity in their cytoplasm; hence, they are not protected by this Ca^{2+}-buffering mechanism. However, most of those cells exhibit simultaneous nuclear translocation of NF-κB colocalized with PARP and undergo apoptosis.

5. Summary

The new findings presented in this work are as follows:

- PARP is upregulated in the motor cortex of ALS patients; this is detected at a protein level by immunoblotting.
- PARP upregulation is primarily localized to the pyramidal cells undergoing degeneration by immunohistochemistry in the motor cortex.
- A milder increase in PARP was noted in other neurons, which usually do not degenerate in ALS.
- A PARP increase was also noted in the DA-ergic neurons of the SN in PD.
- In PD, PARP overactivation coactivates NF-κB, which is a transcription factor for p53 gene expression inducing apoptosis.
- Increased PARP in the microglia reflects its activation, which seems to be necessary to release neurotoxic substances.
- PARP is upregulated in astrocytes, altering their protective function on neurons.
- Autoimmune IgG from ALS targets MNs and is taken up in them. Ultrastructurally, it is bound to the AT of the neuromuscular junction, transported by microtubules to the cell body and accumulated in the RER and in the Golgi apparatus. IgG increases intracellular Ca^{2+}, which also activates PARP.
- In ALS patients, the IgG is localized in the same ultrastructures as in the MNs of mice after passive transfer via ip injection.
- PARP overactivation in the neurons can damage the cells in a cell-autonomous manner and also by activation of the microglia.
- PARP overactivation seems to be a common pathway in the mechanisms of selective neurodegeneration in ALS and PD.
- PARP inhibitors are of potential benefit in the treatment of both diseases.

6. Acknowledgments

I would like to express my gratitude to my supervisor, Professor József Engelhardt M.D., Ph.D. Professor of the Department of Neurology at the University of Szeged, for his scientific guidance and for his support throughout my Ph.D. and medical studies.

I would also like to thank Professor László Vécsei M.D., Ph.D., Chairman of the Department of Neurology at the University of Szeged, for giving me the opportunity to work in his institute.

I am grateful to László Siklós Ph.D. and Izabella Obál M.D., Ph.D. for introducing me to the laboratory techniques and for their help.

I am indebted to Katalin Majtényi M.D., Ph.D. and László Havas M.D. for providing diagnosed *post mortem* human materials for our series of experiment.

I thank to all my colleagues for their assiduous encouragement for me to finish my thesis. I am especially grateful to my family and friends for their love and for their untiring support during my Ph.D. studies.

I express my thanks to various organizations for financial support: grants from the Hungarian Ministry of Health (ETT-0032/2000, ETT-33/2003), the National Scientific Research Fund (OTKA T042858), Fund for Research and Development at the Ministry of Education (FKFP-0032/2000).

7. References

1. Mitsumoto A, Nakagawa Y. DJ-1 is an indicator for endogenous reactive oxygen species elicited by endotoxin. Free Radic Res 35(6): 885–893, 2001.
2. Mandir AS, Przedborski S, Jackson-Lewis V, Wang ZQ, Simbulan-Rosenthal CM, Smulson ME, Hoffman BE, Guastella DB, Dawson VL, Dawson TM. Poly (ADP-ribose) polymerase activation mediates 1-methyl-4-phenyl-1,2,3,6-tetrahydropyridine (MPTP)-induced parkinsonism. Proc Natl Acad Sci USA 96(10): 5774-5779, 1999.
3. Chatha BT, Bernard V, Streit P, Bolam JP. Synaptic localization of ionotropic glutamate receptors in the rat substantia nigra. Neuroscience. 101(4): 1037-51; 2000.
4. Testa CM, Standaert DG, Young AB, Penney JB Jr. Metabotropic glutamate receptor mRNA expression in the basal ganglia of the rat. J Neurosci. 14(5 Pt 2): 3005-18, 1994.
5. Alexi T, Borlongan CV, Faull RL, Williams CE, Clark RG, Gluckman PD, Hughes PE. Neuroprotective strategies for basal ganglia degeneration: Parkinson's and Huntington's diseases. Prog Neurobiol. 60(5): 409-70, 2000. Review.
6. Tapia R, Medina-Ceja L, Pena F. On the relationship between extracellular glutamate, hyperexcitation and neurodegeneration, in vivo. Neurochem Int. 34(1): 23-31, 1999. Review.
7. Ossowska K. The role of excitatory amino acids in experimental models of Parkinson's disease. J Neural Transm Park Dis Dement Sect. 8(1-2): 39-71, 1994. Review.
8. Takeuchi H, Jin S, Wang J, Zhang G, Kawanokuchi J, Kuno R, Sonobe Y, Mizuno T, Suzumura A. Tumor necrosis factor-alpha induces neurotoxicity via glutamate release from hemichannels of activated microglia in an autocrine manner. J Biol Chem. 281 (30): 21362-8, 2006.
9. Kress GJ, Reynolds I. Dopaminergic neurotoxins require excitotoxic stimulation in organotypic cultures. Neurobiol Dis. 20(3): 639-45, 2005.
10. Kaur D, Andersen J. Does cellular iron dysregulation play a causative role in Parkinson's disease? Ageing Res Rev. 3(3): 327-4, 2004.

11. Nagatsu T, Mogi M, Ichinose H, Togari A. Changes in cytokines and neurotrophins in Parkinson's disease J Neural Transm Suppl. (60): 277-90, 2000. Review
12. Wu DC, Jackson-Lewis V, Vila M, Tieu K, Teismann P, Vadseth C, Choi DK, Ischiropoulos H, Przedborski S. Blockade of microglial activation is neuroprotective in the 1-methyl-4-phenyl-1,2,3,6-tetrahydropyridine mouse model of Parkinson disease. J Neurosci. 22(5): 1763-71, 2002.
13. Klegeris A, McGeer PL. Rat brain microglia and peritoneal macrophages show similar responses to respiratory burst stimulants. J Neuroimmunol 53(1): 83-90, 1994.
14. Banati RB, GehrmanJ, Schubert P, Kreutzberg GW. Cytotoxicity of microglia. Glia. 7 (1): 111-8, 1993. Review.
15. Hu S, Sheng WS, Peterson PK, Chao CC. Cytokine modulation of murine microglial cell superoxide production. Glia 13(1): 45-50, 1995.
16. Floden AM, Li S, Combs CK. Beta-amyloid-stimulated microglia induce neuron death via synergistic stimulation of tumor necrosis factor alpha and NMDA receptors. J Neurosci 25(10):2566-75, 2005.
17. Nagatsu T, Sawada M. Inflammatory process in Parkinson's disease: role for cytokines. Curr Pharm Des. 11(8): 999-1016, 2005. Review.
18. Virag L, Szabo C. The therapeutic potential of poly(ADP-ribose)polymerase inhibitors. Pharmacol Rev. 54(3): 375- 429, 2002. Review
19. Hauschildt S, Scheipers P, Bessler WG, Mulsch A. Induction of nitric oxide synthase in L929 cells by tumour-necrosis factor alpha is prevented by inhibitors of poly (ADP-ribose) polymerase. Biochem J. 288 (Pt 1): 255-60, 1992.
20. Le Page C, Sanceau J, Drapier JC, Wietzerbin J. Inhibitors of ADP-ribosylation impair inducible nitric oxide synthase gene transcription through inhibition of NF kappa B activation. Biochem Biophys Res Commun. 243(2): 451-7, 1998.
21. Szabo C, Dawson VL. Role of poly(ADP-ribose)synthetase in inflammation and ischaemia-reperfusion. Trends Pharmacol Sci. 19(7): 287-98. 1998. Review
22. Zingarelli B, Salzman AL, Szabo C. Genetic disruption of poly (ADP-ribose) synthetase inhibits the expression of P-selectin and intercellular adhesion

molecule-1 in myocardial ischemia/reperfusion injury. Circ Res. 83(1): 85-94, 1998.

23. Oliver FJ, Menissier-de Murcia J, Nacci C, Decker P, Andriantsitohaina R, Muller S, de la Rubia G, Stoclet JC, de Murcia G. Resistance to endotoxic shock as a consequence of defective NF-kappaB activation in poly (ADP-ribose) polymerase-1 deficient mice. EMBO J. 18(16): 4446-54, 1999.
24. Kauppinen TM, Swanson RA. Poly(ADP-ribose) polymerase-1 promotes microglial activation, proliferation, and matrix metalloproteinase-9-mediated neuron death. J Immunol. 174(4): 2288-96, 2005.
25. Chiarugi A, Moskowitz MA. Poly(ADP-ribose) polymerase-1 activity promotes NF-kappaB-driven transcription and microglial activation: implication for neurodegenerative disorders. J Neurochem. 85(2): 306-17, 2003.
26. McGeer PL, McGeer EG. Inflammatory processes in amyotrophic lateral sclerosis. Muscle Nerve. 26(4): 459-70, 2002. Review.
27. Llinas R, Sugimori M, Cherksey BD, Smith RG, Delbono O, Stefani E, Appel SH. IgG from amyotrophic lateral sclerosis patients increases current through P-type calcium channels in mammalian cerebellar Purkinje cells and isolated channel protein in lipid bilayer. Proc. Natl. Acad. sci. USA 90(24): 11743-7, 1993.
28. La Bella V, Goodman JC, Appel SH. Increased CSF glutamate following injection of ALS immunoglobulins. Neurology, 48(5): 1270-2, 1997.
29. Kreutzberg GW. Microglia: a sensor for pathological events in the CNS. Trends Neurosci 19(8): 312-8, 1996. Rev.
30. Merill JE, Benveniste EN. Cytokines in inflammatory brain lesions: helpful and harmful. Trends Neurosci. 19(8): 331-338, 1996.
31. Matsumoto Y, Ohmori K, Fujiwara M. Immune regulation by brain cells in the central nervous system: mycroglia but not astrocytes present myelin basic protein to encephalitogenic T cells under in vivo- mimicking conditions. Immunology 76(2): 209-216, 1992.
32. Banati RB, Schubert P, Rothe G, Gehrmann J, Rudolphi K, Valet G, Kreutzberg GW. Modulation of intracellular formation of reactive oxygen intermediates in

peritoneal macrophages and microglia/brain macrophages by propentofylline. J Cereb Blood Flow Metab 14(1): 145-149, 1994.

33. Gehrmann J, Banati R, Wiessner C, Hossmann KA, Kreutzberg GW. Reactive microglia in cerebral ischemia: an early mediator of tissue damage? Neuropathol Appl Neurobiol 21: 277-289, 1995.
34. Smith ME, van der Maesen K, Somera FP. Macrophage and microglial response to cytokines in vitro: phagocytic activity, proteolytic enzyme release, and free radical production. J Neurosci Res. 54(1): 68-78, 1998.
35. Hu S, Chao CC, Khanna KV, Gekker G, Peterson PK, Molitor TW. Cytokine and free radical production by porcine microglia. Clin Immunol Immunopathol 78(1): 93-96, 1996.
36. Shaw PJ, Slade JY, Williams TL, Eggett CJ, Ince PG. Low expression of GluR2 AMPA receptor subunit by human motor neurones. Neuroreport 10(2): 261-265, 1999.
37. Williams TL, Day NC, Ince PG, Kamboj RK, Shaw PJ. Calcium- permeable alpha-amino -3- hydoxy-5-methyl-4-isoxazole propionic acid receptors: a molecular determinant of selective vulnerability in amyotrophic lateral sclerosis. Ann. Neurol. 42(2): 200-207, 1997.
38. Rothstein JD, Van Kammen M, Levey AI, Martin LJ, Kuncl RW. Selective loss of glial glutamate transporter GLT-1 in amyotrophic lateral sclerosis. Ann Neurol. 38(1): 73-84, 1995.
39. Brujin LI, Becher MW, Lee MK, Anderson KL, Jenkins NA, Copeland NG, Sisodia SS, Rothstein JD, Borchelt DR, Price DL, Cleveland DW. ALS- linked SOD1 mutant G85R mediates damage to astrocytes and promotes rapidly progressive disease with SOD 1-containing inclusions. Neuron 18: 327-338, 1997.
40. Ferrante RJ , Browne SE, Shinobu LA, Bowling AC, Baik MJ, MacGarvey U,Kowall NW, Brown RhJr, Beal MF. Evidence of increased oxidative damage in both sporadic and familial amyotrophic lateral sclerosis. J. Neurochem. 69(5): 2064-2074, 1997.

41. Crow JP, Ye YZ, Strong M, Kirk M, Barnes S, Beckman JS. Superoxide dismutase catalyzes nitration of tyrosines by peroxynitrite in the rod and head domains of neurofilament-L. J Neurochem 69(5): 1945-1953, 1997.
42. Rabizadeh S, Gralla EB, Borchelt DR, Gwinn R, Valentine JS, Sisodia SS, Wong P, lee M, Hahn H, Bredesen DE. Mutations associated with amyotrophic lateral sclerosis convert superoxide dismutase from an antiapoptotic gene to a proapoptotic gene: studies in yeast and neural cells. Proc Natl Acad Sci USA 92(7): 3024-3028, 1995.
43. Siklos L, Engelhardt JI, Harati Y, Smith RG, Joo F, Appel SH. Ultrastructural evidence for altered calcium in the motor nerve terminals in amyotrophic lateral sclerosis. Ann Neurol 39(2): 203-216, 1996.
44. Siklos L, Engelhardt JI, Alexianu ME, Gurney ME, Siddique T, Appel SH. Intracellular calcium parallels motoneuron degeneration in SOD-1 mutant mice. J Neuropath Exp Neurol 57(6): 571-587, 1996.
45. Ackerley S, Grierson AJ, Brownlees J, Thornhill P, Anderton BH, Leigh PN, Shaw CE, Miller CC. Glutamate slows axonal transport of neurofilaments in transfected neurons. J Cell Biol 150(1): 165-76, 2000.
46. Chou SM, Wang HS, Komai K. Colocalization of NOS and SOD1 in neurofilament accumulation within motor neurons of amyotrophic lateral sclerosis: an immunohistochemical study. J Chem Neuroanat. 10(3-4): 249-58, 1996.
47. Karczewski JM, Peters JG, Noordhoek J. Prevention of oxidant induced cell death in Caco-2 colon carcinoma cells after inhibition of poly(ADP-ribose) polymerase and Ca^{2+} chelation: involvement of a common mechanism. Biochem Pharmacol. 57(1): 19-26, 1999.
48. Garthwaite G, Goodwin DA, Batchelor AM, Leeming K, Garthwaite J. Nitric oxide toxicity in CNS white matter: an in vitro study using rat optic nerve. Neuroscience 109(1): 145-55, 2002.
49. Schraufstatter IU, Hinshaw DB, Hyslop PA, Spragg RG, Cochrane CG. Oxidant injury of cells. DNA strand-breaks activate polyadenosine diphosphate-ribose polymerase and lead to depletion of nicotinamide adenine dinucleotide. J Clin Invest 77(4): 1312-20, 1986.

50. Zhang J, Dawson WL, Dawson TM, Snyder SH. Nitric oxide activation of poly (ADP-ribose) synthetase in neurotoxicity. Science 263(5147): 687-89, 1994.
51. Ha HC, Snyder SH. Poly (ADP-ribose) polymerase is a mediator of necrotic cell death by ATP depletion. Proc Natl Acad Sci USA 96(24): 13978-82, 1999.
52. Schraufstatter IU, Hyslop PA, Hinshaw DB, Spragg RG, Sklar LA, Cochrane CG. Hydrogen peroxide- induced injury of cells and its prevention by inhibitors of poly (ADP-ribose) polymerase. Proc Natl Acad Sci USA 83(13): 4908-12, 1986.
53. Wallis RA, Panizzon KL, Henry D, Wasterlain CG. Neuroprotection against nitric oxide injury with inhibitors of ADP-ribosylation. Neuroreport 5(3): 245-48, 1993.
54. Miller RG, Munsat TL, Swash M, Brooks BR. Consensus guidelines for the design and implementation of clinical trials in ALS. World Federation of Neurology Committee on Research. J Neurol Sci 169(1-2): 2-12, 1999.
55. Somogyi P, Takagi H. A note on the use of picric acid-paraformaldehyde-glutaraldehyde fixative for correlated light and electron microscopic immunocytochemistry. Neuroscience 7(7): 1779-1783, 1982.
56. Hassa PO and Hottiger MO. A role of poly (ADP-ribose) polymerase in NF-κB transcriptional activation. Biol Chem 380(7-8): 953-959, 1999.
57. Szabo C. Role of poly(ADP-ribose)synthetase in inflammation. Eur J Pharmacol. 350(1): 1-19, 1998.
58. Carson DA, Seto S, Wasson DB, Carrera CJ. DNA strand breaks, NAD metabolism, and programmed cell death. Exp Cell Res 164(2): 273-81, 1986.
59. Ying W, Alano CC, Garnier P, Swanson RA. NAD+ as a metabolic link between DNA damage and cell death. J Neurosci 79(1-2): 216-23, 2005.
60. Kim SH, Henkel JS, Beers DR, Sengun IS, Simpson EP, Goodman JC, Engelhardt JL, Siklos L, Appel SH. PARP expression is increased in astrocytes but decreased in motor neurons in the spinal cord of sporadic ALS patients. J Neuropathol Exp Neurol 62(1): 88-103, 2003.
61. Kim SH, Engelhardt JI, Henkel JS, Siklos L, Soos J, Goodman JC, Appel SH. Widespread increased expression of the DNA repair enzyme PARP in brain in ALS. Neurology. 62 (2): 319-22, 2004.

62. Cleveland DW, Liu J. Oxidation versus aggregation - how do SOD1 mutants cause ALS? Nat Med 6: 1320-1321, 2000.
63. Sasaki S, Iwata M. Impairment of fast axonal transport in the proximal axons of anterior horn neurons in amyotrophic lateral sclerosis Neurology. 47(2): 535-540, 1996.
64. Wang H, Shimoji M, Yu SW, Dawson TM, Dawson VL. Apoptosis inducing factor and PARP-mediated injury in the MPTP mouse model of Parkinson's disease. Ann N Y Acad Sci 991: 132-9, 2003.
65. Love S, Barber R, Wilcok G. Increased poly (ADP-ribosyl) ation of nuclear proteins in Alzheimer's disease. Brain 122:247-253, 1999.
66. Endes M, Wang ZQ, Namura S, Waeber C, Mosskowitz MA. Ischemic brain injury is mediated by the activation of poly(ADP-ribose)polymerase. J Cereb Blood Flow Metab 17(11): 1143-1151, 1997.
67. Scott GS, Jakeman LB, Stokes BT, Szabo C. Peroxynitrite production and activation of poly (ADP-ribose) synthetase in spinal cord injury. Ann Neurol 45: 120-124, 1999.
68. Denk A, Wirth T and Baumann B. NF-κB transcription factors: critical regulators of hematopoesis and neuronal survival. Cytokine Growth Factor Rev. 11(4): 303-320, 2000.
69. de Erausquin GA, Hyrc K, Dorsey DA, Mamah D, Dokucu M, Mascó DH et al. Nuclear translocation of nuclear transcription factor - κB by α-amino-3-hydroxy-5-methyl-isoxazolepropionic acid receptors leads to transcription of p53 and cell death in dopaminergic neurons. Mol Pharmacol 63(4): 784-790, 2003.
70. Jellinger KA, Stadelmann C. Mechanisms of cell death in neurodegenerative disorders. J Neural Transm Suppl. 59: 95-114, 2000.
71. Mattson MP, Culmsee C, Yu Z, Camandola S. Roles of nuclear factor kappaB in neuronal survival and plasticity. J Neurochem 74(2): 443-456, 2000.
72. Lee HJ, Kim SH, Kim KW, Um JH, Lee HW, Chung BS Kang CD. Antiapoptotic role of NF-κB in auto-oxidized dopamine-induced apoptosis of PC12 cells. J Neurochem 76(2), 602-609, 2001.
73. Hunot S, Brugg B, Ricard D, Michel PP, Muriel MP, Ruberg M, FaucheuxíBA, Agid Y, Hirsch EC. Nuclear translocation of NF-κB is increased in

dopaminergic neurons of patients with Parkinson disease. Proc Natl Acad Sci USA 94(14): 7531- 7536,1997.

74. Tewari M, Quan LT, O'Rourke K, Desnoyers S, Zeng Z, Beidler DR, Poirier GG, Salvesn GS, Dixit VM. Yama/CPP32 beta, a mammalian homolog of CED-3, is a CrmA-inhibitable protease that cleaves the death substrate poly (ADP-ribose) polymerase. Cell 81(5): 801-809, 1995.
75. Colton CA, Gilbert DL. Production of superoxide anions by CNS macrophage, the microglia. FEBS Lett 223(2): 284-288, 1987.
76. Bal-price A, Matthias A, Brown GC. Stimulation of the NADPH oxidase in activated rat microglia removes nitric oxide but induces peroxynitrite production. J Neurochem. 80(1): 73-80, 2002.
77. Barger SW, Basile AS. Activation of microglia by secreted amyloid precursor protein evokes release of glutamate by cystine exchange and attenuates synaptic function. J Neurochem 76(3): 846-54, 2001.
78. Chao CC, Hu S, Peterson PK. Modulation of human microglial cell superoxide production by cytokines. J Leukoc Biol. 58(1): 65-70, 1995.
79. Tanaka J, Toku K, Zhang B, Ishihara K, Sakanaka M, Maeda N. Astrocytes prevent neuronal death induced by reactive oxygen and nitrogen species. Glia 28(2): 85-96, 1999.
80. Desagher S, Glowinski J, Permont J. Astrocytes protect neurons from hydrogen peroxide toxicity. J Neurosci 16(8): 2553-62, 1996.
81. Lindsay RM. Adult rat brain astrocytes support survival of both NGF-dependent and NGF- insensitive neurones. Nature 282: 80-82, 1979.
82. Hori O, Matsumoto M, Kuwabara K, et al. Exposure of astrocytes to hypoxia/ reoxigenation enhances expression of glucose- regulated protein 78 facilitating astrocyte release of the neuroprotective cytokine interrleukin 6. J Neurochem 66(3): 973-79), 1996.
83. Thoenen H, Hughes RA, Sendtner M. Trophic support of motoneurons: physiological, pathophysiological, and therapeutic implications. Exp Neurol 124(1): 47-55, 1993.

84. Alexianu ME, Ho BK, Mohamed AH, LaBella V, Smith RG, Appel SH. The role of calcium binding proteins in selective motoneuron vulnerability in amyotrophic lateral sclerosis. Ann Neurol 36(6): 848-858, 1994.

85. Bowling AC, Schulz JB, Brown RH Jr, Beal MF. Superoxide dismutase activity, oxidative damage, and mitochondrial energy metabolism in familial and sporadic amyotrophic lateral sclerosis. J Neurochem 61 (6): 2322-2325, 1993.

86. Shaw PJ, Ince PG, Falkous G Mantle D. Oxidative damage to protein in sporadic motor neuron disease spinal cord. Ann Neurol 38(4): 691-695, 1995.

87. Abe K, Pan LH, Watanabe M, Kato T, Itoyama Y. Induction of nitrotyrosine-like immunoreactivity in the lower motor neuron of amyotrophic lateral sclerosis. Neurosci Lett.199(2): 152-154, 1995.

88. Beal MF, Ferrante RJ, Browne SE, Matthews RT, Kowall NW, Brown RH Jr. Increased 3-nitrotyrosine in both sporadic and familial amyotrophic lateral sclerosis. Ann Neurol 42(4): 646-654, 1997.

89. Tohgi H, Abe T, Yamazaki K, Murata T, Ishizaki E, Isobe C. Remarkable increase in cerebrospinal fluid 3-nitrotyrosine in patients with sporadic amyotrophic lateral sclerosis. Ann Neurol 46(1): 129-131, 1999.

90. Robberecht W, Sapp P, Viaene MK, Rosen D, McKenna-Yasek D, Haines J, Horvitz R, Theys P, Brown RhJr. Cu/Zn superoxide dismutase activity in familial and sporadic amyotrophic lateral sclerosis. J Neurochem 62(1): 387-5, 1994.

91. Pedersen WA, Fu W, Keller JN, Markesbery WR, Appel S, Smith RG, Kasarskis E, Mattson MP. Protein modification by the lipid peroxidation product 4-hydroxynonenal in the spinal cords of amyotrophic lateral sclerosis patients. Ann Neurol 44(5): 819-824, 1998.

92. Smith RG, Henry YK, Mattson MP, Appel SH. Presence of 4-hydroxynonenal in cerebrospinal fluid of patients with sporadic amyotrophic lateral sclerosis. Ann Neurol 44(4): 696-699, 1998.

93. Fitzmaurice PS, Shaw IC, Kleiner HE, Miller RT, Monks TJ, Lau SS, Mitchell JD, Lynch PG. Evidence for DNA damage in amyotrophic lateral sclerosis. Muscle Nerve. 19(6): 797-798, 1996.

94. Bogdanov M, Brown RH Jr, Matson W, Smart R, Hayden D, O'Donnell H, Flint Beal M, Cudkowicz M. Increased oxidative damage to DNA in ALS patients. Free Radic Biol Med 29(7): 652-658, 2000.

95. Alexianu ME, Mohamed AH, Smith RG, Colom LV, Appel SH. Apoptotic cell death of a hybrid motoneuron cell line induced by immunoglobulins from patients with amyotrophic lateral sclerosis. J Neurochem 63(6): 2365-2368, 1994.

96. Parkes AB, Rickards CR, Rees P, Scanlon MF. Cytotoxic changes in A172 glioblastoma cells exposed to serum IgG from patients with motor neurone disease. J Neurol Sci 129(Suppl): 136-137, 1995.

97. Pullen AH, Demestre M, Howard RS, Orell RW. Passive transfer of purified IgG from patients with amyotrophic lateral sclerosis to mice results in degeneration of motor neurons accompanied by Ca^{2+} enhancement. Acta Neuropathol 107(1): 35-46, 2004.

98. Appel SH, Engelhardt JI, Garcia J, Stefani E. Immunoglobulins from animal models of motor neuron disease and from human amyotrophic lateral sclerosis patients passively transfer physiological abnormalities to the neuromuscular junction. Proc Natl Acad Sci USA 88(2): 647-651, 1991.

99. Grassi C, Martire M, Altobelli D, Azzena GB, Preziosi P. Characterization of Ca^{2+}-channels responsible for K^{+}-evoked (^{3}H) noradrenaline release from rat brain cortex synaptosomes and their response to amyotrophic lateral sclerosis IgGs. Exp Neurol 159: 520-527, 1999.

100. Appel SH, Beers D, Siklos L, Engelhardt JI, Mosier DR. Calcium: The Darth Vader of ALS. Amyotroph Lateral Scler Other Motor Neuron Disord. 2Suppl 1: S47-54, 2001.

101. Appel SH, Smith RG, Alexianu M, Siklos L, Engelhardt JI, Colom LV, Stefani E. Increased intracellular calcium triggered by immune mechanisms in amyotrophic lateral sclerosis. Clin Neurosci 3(6): 368-374, 1996.

102. Mohamed HA, Mosier DR, Zou LL, Siklos L, Alexianu ME, Engelhardt JI, Beers DR, Le WD, Appel SH. Immunoglobulin Fcγ receptor promotes immunoglobulin uptake, immunoglobulin-mediated calcium increase, and neurotransmitter release in motor neurons. J Neurosci Res 69(1): 110-116, 2002.

103. Breittmayer JP, Berthe P, Cousin JL, Bernard A, Aussel C. CD3 monoclonal antibodies evoke the same cytochrome P450-regulated capacitative entry of calcium as thapsigargin in Jurkat T cells. Cell Immunol 152(1): 143-151, 1993.
104. Binet S, Meininger V. Modifications of microtubule proteins in ALS nerve precede detactable histologic and ultrastructural changes. Neurology 38(10): 1596-1600, 1988.
105. Wehland J, Henkart M, Klausner R, Sandoval IV. Role of microtubules in the distribution of the Golgi apparatus: effect of taxol and microinjected anti-α-tubulin antibodies. Proc Natl Acad Sci USA 80(14): 4286-4290, 1983.
106. Stieber A, Chen Y, Wei S, Mourelatos Z, Gonatas J, Okamoto K, Gonatas NK. The fragmented neuronal Golgi apparatus in amyotrophic lateral sclerosis includes the trans-Golgi-network: functional implications. Acta Neuropathol 95(3): 245-253, 1998.
107. Hurd DD, Saxton WM. Kinesin mutations cause motor neuron disease phenotypes disrupting fast axonal transport in Drosophila. Genetics 144(3): 1075-1085, 1996.
108. Hirokawa N, Hisanaga S, Shiomura Y. MAP2 is a component of crossbridges between microtubule and neurofilaments in the neuronal cytoskeleton: quick-free, deep-etch immunoelectron microscopy and reconstitution studies. J Neurosci 8(8): 2769-2779, 1988.
109. Engelhardt JI, Siklos L, Komuves L, Smith RG, Appel SH. Antibodies to calcium channels from ALS patients passively transferred to mice selectively increase intracellular calcium and induce ultrastructural changes in motoneurons. Synapse 20(3): 185-199, 1995.
110. Pullen AH, Humphreys P. Ultrastructural analysis of spinal motoneurones from mice treated with IgG from ALS patients, healthy individuals, or disease controls. J Neurol Sci 180(1-2): 35-45, 2000.
111. Obal I, Soos J, Jakab K, Siklos L, Engelhardt JI. Recruitment of activated microglia cells in the spinal cord of mice by ALS IgG. Neuroreport 12(1-2): 2449-52, 2001.
112. Upender MB, Naegele JR. Activation of microglia during developmentally regulated cell death in the cerebral cortex. Dev Neurosci 21(6): 491-505, 1999.

113. Jenner P. Oxidative stress in Parkinson's disease. Ann Neurol 53 Suppl 3: S26-S36; discussion S36-S38, 2003.

114. McGeer PL, McGeer EG. Inflammation and neurodegeneration in Parkinson's disease. Parkinsonism and relat disorder 10 Suppl 1; S3-7. Review.

115. Hald A, Lotharius J. Oxidative stress and inflammation in Parkinson's disease: is there a causal link? Exp Neurol 193(2): 279-290, 2005.

116. Hardman CD, McRitchie DA, Halliday GM, Cartwright HR, Morris JG. Substantia nigra pars reticulata neurons in Parkinson's disease. Neurodegeneration 5(1): 49-55, 1996.

117. Dekkers J, Bayley P, Dick JR, Schwaller B, Berchtold MW, Greensmith L. Over-expression of parvalbumin in transgenic mice rescues motoneurons from injury-induced cell death. Neuroscience 123(2): 459-466, 2004.

118. Beers DR, Ho BK, Siklós L, Alexianu ME, Mosier DR, Mohamed AH, OtsukaY, Kozovska ME, McAlhany RE, Smith RG, Appel SH. Parvalbumin overexpression alters immune-mediated increases in intracellular calcium, and delays disease onset in transgenic model of familial amyotrophic lateral sclerosis. J Neurochem 79(3): 499-509, 2001.